A MULTI-DECADAL PRECIPITATION EVALUATION FOR NAMIBIA USING SATELLITE, MODEL, AND GROUND-BASED DATA

A Thesis

by

RHETT JON DOURIS

Submitted to the Office of Graduate and Professional Studies of
Texas A&M University
in partial fulfillment of the requirements for the degree of

MASTER OF SCIENCE

Chair of Committee,	Oliver Frauenfeld
Committee Members,	Anita Rapp
	E. Brendan Roark
Head of Department,	David Cairns

August 2019

Major Subject: Geography

ABSTRACT

Precipitation in southern Africa exhibits high variability with rain often falling in an intense deluge or not at all. Considerable research has gone into understanding what drives precipitation in southern Africa and how it can be better predicted. Where past research has usually evaluated southern Africa in general or South Africa in particular, this study looks at precipitation in Namibia, a country with a unique climate regime. The first objective of this thesis seeks to identify a long-term precipitation product that accurately represents precipitation over Namibia. The second objective is to utilize the long-term product to create precipitation climatologies and determine trends at different scales. The final objective identifies relationships between precipitation in Namibia and global teleconnections, and how those global teleconnections drive precipitation in Namibia.

Three long-term precipitation products, Climate Prediction Center Unified Gauge-based Analysis of Global Daily Precipitation, Climatic Research Unit Timeseries Version 4.01, and European Centre for Medium-Range Weather Forecasts Reanalysis-Interim (ERA), are compared against Tropical Rainfall Measuring Mission 3G68Land, a satellite-based product considered here to represent observed precipitation. Using five metrics and three different analyses, ERA is identified as the best long-term precipitation product.

ERA is used to create climatologies that highlight the beginning (October), peak (January), and end (April) of the Namibian rainy season, as well as quantify mean

annual precipitation. Trends show increasing annual precipitation in Namibia, as well as positive monthly precipitation trends in December, January, and March.

The drivers of precipitation in Namibia via global teleconnections are identified using both the original ERA precipitation, and the first two principal components of Namibian precipitation. Monthly, seasonal, and annual time scales at thirteen lag times are compared. January and February precipitation positively correlates to the Southern Oscillation Index, while February precipitation negatively correlates to the Pacific Decadal Oscillation. The results suggest that global teleconnections in the Pacific have the greatest influence on Namibia's precipitation regime.

DEDICATION

This thesis is dedicated to my mother, Tammy, my sister, Steele, and my grandparents, Claire and John. None of this would have been possible without you. Thank you for always being there for me, I love you all so much.

ACKNOWLEDGEMENTS

I would like to thank my committee chair Dr. Frauenfeld, and my committee members, Dr. Roark, and Dr. Rapp, for their counsel and support. I would like to give particular thanks to Dr. Frauenfeld for his extensive time, advice, and assistance which were invaluable. He lighted my pathway even in times of considerable darkness and doubt.

Thanks also go to the graduate students of the Texas A&M Department of Geography. As someone once said “graduate school is an ordeal”, and the process is made that much better by the incredible friends you make along the way. I want to give particular thanks to Ellen Bartow-Gillies, Cesar Castillo, Victoria Ford, Carl Green, Kelci Miller, and John Schiff for their incredible friendship over the past few years.

Finally, I want to give my greatest gratitude to my mother and sister, Tammy and Steele Douris. They were always there for me when I needed guidance... Or the occasional proof reading. Their love, support, and patience kept me going even when the going got tough. Thank you.

CONTRIBUTORS AND FUNDING SOURCES

Contributors

This work was supervised by a thesis committee consisting of Professor Frauenfeld (advisor), and Professor Roark of the Department of Geography and Professor Rapp of the Department of Atmospheric Sciences. All work conducted for the thesis was completed by the student independently.

Funding Sources

Graduate study was supported by a graduate merit fellowship from The College of Geosciences at Texas A&M University and a departmental assistantship from the Department of Geography at Texas A&M University.

NOMENCLATURE

20CRv2	NOAA-CIRES 20th Century Reanalysis V2
CMORPH	CPC Morphing
CPC	Climate Prediction Center Unified Gauge-based Analysis of Global Daily Precipitation
CRU	Climatic Research Unit Timeseries Version 4.01
ENSO	El Niño – Southern Oscillation
ERA	European Centre for Medium-Range Weather Forecasts Reanalysis-Interim
GFS	General Forecast System
GPCP	Global Precipitation Climatology Project
HadISST	Hadley Centre Global Sea Ice and Sea Surface Temperature
IOD	Indian Ocean Dipole
MAE	Mean Absolute Error
ME	Mean Error
NAO	North Atlantic Oscillation
NCEP	National Environmental Prediction Center
ONI	Oceanic Niño Index
PC	Principal Component
PCA	Principal Component Analysis
PDO	Pacific Decadal Oscillation
PR	Precipitation Radar

RMSE	Root Mean Squared Error
SICZ	South Indian Convergence Zone
SIOD	Subtropical Indian Ocean Dipole
SLP	Sea Level Pressure
SO	Southern Oscillation
SOI	Southern Oscillation Index
SST	Sea Surface Temperature
TRMM	Tropical Rainfall Measuring Mission
TSA	Tropical Southern Atlantic Index

TABLE OF CONTENTS

Page

LIST OF FIGURES

Page

LIST OF TABLES

Page

1. INTRODUCTION AND LITERATURE REVIEW

1.1. Overview

The location, timing, and quantity of precipitation across arid and semi-arid regions have been an important topic of study for decades (Kokot, 1948, Tyson and Dyer, 1978, Lindesay et al., 1986). A lack of precipitation over a semi-arid region can mean the difference between a successful growing season and a failed one. Too much precipitation in too short a time period can have an equally destructive effect. While precipitation is important for industry and agriculture, it also plays a key role for wildlife. The arrival and departure of seasonal precipitation is known to have a direct impact on the migration of numerous species, even when the precipitation event is tens of kilometers away (Leggett, 2006, Garstang et al., 2014). The relationship between precipitation and wildlife, particularly the relationship between precipitation and the migration of elephants, engendered this study of precipitation in Namibia.

Namibia is a sparsely populated country that lies almost entirely between 17° - 29°S and 11° - 21° E, with the Caprivi Strip in the northeastern corner of the country extending out to 25°E. The Namibian coastline is covered by the Namib Desert, which stretches from Angola in the north to South Africa in the south. The combination of the low Benguela Current from the Antarctic and the high pressure system caused by sinking air from the Hadley cell are the primary stimuli behind the Namib Desert's climate (Muller et al., 2008). This combination of high pressure and low sea surface temperatures (SST) has created a desert that is entirely unique. While the Namib Desert

bears some resemblance to the Atacama Desert of South America, it does not experience a rain shadow effect to inhibit convection. The unusual nature of Namibia's climate proved to be an important factor in choosing the location for this study, because while there are numerous studies that discuss precipitation across "southern Africa" as a whole, as is discussed later in this section, very little research has been done that only looks at the country of Namibia.

Regardless of location, southern Africa in general experiences considerable precipitation variability throughout the year. The dry season begins approximately in February and March and extends through the austral winter. Precipitation returns once again to southern Africa in October and November and continues on through the austral summer. With high precipitation variability, droughts in Namibia occur with relatively high frequency (Landman et al., 2009). Annual precipitation totals over Namibia can range from 20 mm in the coastal region, to 600 mm along the northeastern border with Angola (Nicholson, 2000). Southern African rainfall in the austral summer is known to primarily be the result of deep convection that results in short, high intensity precipitation events (Cretat et al., 2012).

1.2. Precipitation in Southern Africa

The study of precipitation in southern Africa dates as far back as the 19th Century (Tripp, 1888), thus understanding precipitation in southern Africa has been a topic of interest for over a century. Tyson et al. (1975) used gauge data from the modern countries of South Africa, Lesotho, and Swaziland, to argue that precipitation had not been decreasing over the last 100 years, but that there were noticeable oscillations in the

precipitation. Dyer (1979) performed three principal component analyses (PCA) on precipitation in southern Africa, the Southern Oscillation Index (SOI), and the Australian subtropical high pressure belt, followed by a step-wise regression analysis. He found that depending on the latitude of the high pressure belt, precipitation on the eastern coast of South Africa increased or decreased, while changes in the SOI had no effect on precipitation. In the decade that followed, considerable research was performed that evaluated and contradicted the Dyer (1979) findings, with numerous studies investigating the relationship between the precipitation in southern Africa (and Africa in general) and coupled ocean-atmosphere systems, particularly the El Niño – Southern Oscillation (ENSO) (Lindesay et al., 1986, Nicholson and Entekhabi, 1986, Lindesay, 1988, Vanheerden et al., 1988). The prevailing consensus by the end of the 1980s appeared to be that ENSO was influencing precipitation in southern Africa (Lindesay, 1988, Vanheerden et al., 1988). For most of the studies, the data being evaluated were based only on gauge measurements from stations in South Africa.

Lindesay (1988) found that the high phase of the Southern Oscillation (SO) is correlated with above average precipitation over southern Africa while the low phase correlates with below average precipitation. This relationship was found to be strongest during the late summer months (January – March) in central South Africa. A much weaker correlation was found in the early summer months (October – December) and with some parts of southwestern South Africa actually having the opposite correlation. The study was expanded to consider a separate time period, from 1820-1920, and found the same relationship between southern African precipitation and ENSO (Lindesay and

Vogel, 1990). The finding led Lindesay and Vogel (1990) to conclude that the precipitation - SO relationship has remained the same for the past 200 years. The ENSO signal was later found to have the greatest effect on precipitation in southern Africa depending on SST in the Indian and Atlantic Oceans (Nicholson and Kim, 1997). Later research by (Nicholson and Selato, 2000) would focus on the La Niña phase of ENSO and its influences on rainfall across Africa. As expected based on past research, it was found that precipitation would increase on the western coast of Africa (particularly Namibia) during La Niña, especially in the latter half of the phase. One theory put forward by which the ENSO SST anomaly was thought to connect to precipitation over Africa was traced to an area termed the South Indian Convergence Zone (SICZ), a land-based convergence zone positioned off the southeastern side of southern Africa (Cook, 2000). Cook (2000) found that the SICZ would move depending upon the SST anomalies of ENSO. During an El Niño phase, the SICZ would shift towards the northeast, thus moving away from southern Africa and decreasing precipitation. When ENSO was in the La Niña phase, the SICZ would shift towards the southwest and bring increased precipitation (Cook, 2001). The SICZ is generally only active during the austral summer.

In addition to ENSO affecting precipitation in southern Africa, a positive correlation between SSTs off the eastern and western coasts of southern Africa and precipitation was found to be quite strong, especially when the ENSO signal was removed (Walker, 1990). While not nearly as well-known as ENSO in the Pacific Ocean, the southern Atlantic Ocean is understood to have an SST oscillation that

resembles ENSO. This Benguela Niño was first categorized by Shannon et al. (1986), where the warm phase was found to increase precipitation on the western coast of Namibia and Angola (Rouault et al., 2003). The understanding of Rouault et al. (2003) seems to concur with the assessment of Walker (1990), which at the time did not classify high SST in the Benguela current as the warm phase of a Benguela Niño. Nicholson and Entekhabi (1987) also found a relationship between the SST in the Benguela current and precipitation on the western coast. At that time however, the relationship was thought to be connected to ENSO. Regardless, it can be concluded that Atlantic Ocean SST affects precipitation, even if the oscillation driving that relationship was obscure.

In the Indian Ocean, a different set of factors was found to impact precipitation over southern Africa. High SST in the southwest Indian Ocean was positively correlated to precipitation over the eastern part of South Africa and a decrease in precipitation correlated to low SST (Reason and Mulenga, 1999). The correlation to SST in the Indian Ocean can also be connected to the Indian Ocean Dipole (IOD) (Saji et al., 1999). A phenomenon first described in 1999, the IOD is an ocean-atmosphere interaction based on an SST oscillation in the Indian Ocean. Saji et al. (1999) found that above normal SST in the west Indian Ocean coincided with below normal SST in the southeast Indian Ocean. This SST oscillation was then compared to precipitation patterns in the regions surrounding the Indian Ocean (East Africa and Indonesia), and a correlation was found with high precipitation over East Africa and low precipitation over Indonesia (Saji et al., 1999).

Though a connection had been made between the IOD and precipitation in East Africa, Reason (2001) found that the eastern coast of South Africa experiences an increase in precipitation when the IOD warm phase is occurring. Reason (2002) found that the closer the SST anomaly is to the southeastern coast of Africa, the more it would affect precipitation over southeastern Africa. Neither study discussed whether the IOD affected precipitation in southwestern Africa. Indian Ocean SST anomalies are thought to also affect the movement of the SICZ, much in the same way as ENSO (Cook, 2000, Cook, 2001, Dieppois et al., 2016).

There have been recent studies that have looked at the phenomenon now referred to as ENSO Modoki, a related though different cycle. The ENSO Modoki cycle was identified in the first decade of the 2000s (Ashok et al., 2007, Weng et al., 2007). The location of the SST anomaly was found to be distinctly different from the regular ENSO, thus a new index was created to represent the ENSO Modoki. The creation of this new index has allowed researchers to look at how different the regular ENSO is from the ENSO Modoki in southern Africa. Ratnam et al. (2014) suggests that the El Niño phase of both ENSO and the ENSO Modoki lead to anomalously low precipitation over southern Africa. The methods by which the anomalies are connected to precipitation in southern Africa are somewhat different due to the different locations of the SST anomalies, but the difference in the precipitation anomaly over southern Africa between the two events is not significant.

Researchers have now turned to establishing which variables have the greatest effect on precipitation and what that effect might be based on multiple interacting

variables. Hoell et al. (2017) found that when ENSO and the Subtropical Indian Ocean Dipole (SIOD) were in the same phase, El Niño – positive SIOD/La Niña – negative SIOD, they would cancel out one another's influence on precipitation. Yet, if they were in opposing phases, El Niño – Negative SIOD would lead to more extreme dry years and La Niña – Positive SIOD would lead to more extreme wet years over southern Africa. Hoell and Cheng (2018) further elucidated the relationship between SIOD and ENSO, by demonstrating that the mechanism that delivers increased or decreased precipitation over southern Namibia, an anomalous lower tropospheric cyclone or anticyclone, respectively, is the same regardless of whether the driver is SIOD, ENSO or both. To conclude, almost all the research that has been done in southern Africa looks at the entire region, or just the country of South Africa. The research has found numerous relationships between various global teleconnections, but almost none of them are tied directly to Namibia. Because Namibia has a climate regime that is distinct from the rest of southern Africa, it is important to understand how teleconnections such as IOD, and ENSO, affect Namibia in particular.

1.3. Precipitation Products over Namibia

With the lowest population density of any country on the African continent and a civil war that spanned over twenty years, Namibia suffers from a sparsity of precipitation data (Stanley, 2002, Zhang et al., 2013). While the country of South Africa has a relatively sizable gauge network, much of the rest of southern Africa does not. As a substitute for the small gauge network in Namibia, the Tropical Rainfall Measuring Mission (TRMM) satellite provides an alternative observational product for Namibia.

The TRMM precipitation radar (PR) provides better estimates of precipitation than passive microwave sensors, including the TRMM Microwave Imager sensor. The precipitation product provided by TRMM covers a short time period, thus for longer studies, other products are necessary. This necessitates the use of gridded global products that may not accurately represent precipitation over smaller regions. Before these products can be use over regions such as Namibia, a careful assessment is necessary to make sure the product is properly representing the precipitation regime.

The comparison of precipitation products has been performed for West Africa in a number of studies (Lamptey, 2008, Akinsanola et al., 2017). Similar comparisons have also been done for other countries around the world using various methods (Costa and Foley, 1998, Janowiak et al., 1998, Zhao and Fu, 2006, Juarez et al., 2009, Ma et al., 2009). Precipitation was compared by Thorne et al. (2001) over southern Africa, looking primarily at the methodologies that were used to create the datasets and only considering a seven month period. However, while a comparison of precipitation products was done for southern Africa in general, there is no comparison to find the best precipitation product for use for Namibia. With the downward limb of the Hadley Cell positioned directly over the country and the cold Benguela Current providing almost no moisture, Namibia has a unique climate. Even the closest analog, the Atacama Desert along the western coast of South America, is different. With no high mountain range to the east, Namibia has very limited orographic influences. Analyzing precipitation over a location as unique as Namibia is thus of particular interest.

1.4. Research Goal and Objectives

The research goal of this thesis is to quantify Namibia's precipitation regime and identify its drivers through global teleconnections. The first objective of this thesis is to find the long-term dataset that best captures precipitation variability over Namibia. To do this, a short-term satellite product, TRMM, is used to identify which of the numerous long-term products is most reliable. Products based on interpolated station data, modeled (reanalysis) precipitation, and blended gauge-satellite-modeled data will be assessed. Once the best long-term product is identified, the second objective will create climatologies for Namibia at different timescales (monthly, seasonal, yearly) that show the spatial and temporal variability of precipitation in Namibia. Finally, the third objective will identify what global climatic drivers and teleconnections have the greatest influence on precipitation variability over Namibia.

2. DATA

2.1. Gridded Datasets

2.1.1. Satellite Precipitation Observations

The TRMM satellite was developed to study precipitation over the tropics (Kummerow et al., 1998) and sub-tropics. This thesis utilizes the TRMM 3G68Land precipitation dataset provided by the satellite's PR sensor over Namibia. The PR sensor has been found to provide accurate precipitation readings over regions where ground radar is not available. The 3G68Land product also provides data from the TRMM Microwave Imager sensor, however only PR sensor data were used due to the concern that the TMI sensor would overestimate convective rainfall (McCollum et al., 2002, McCollum and Ferraro, 2003). The daily 3G68Land data, available from 1998 to 2014 at a 0.1° by 0.1° spatial resolution, were resampled to a monthly temporal resolution.

2.1.2. Gauge-Based Blended Precipitation

The Climate Prediction Center Unified Gauge-based Analysis of Global Daily Precipitation (CPC) is a blended dataset that is primarily based upon gauge data (Xie et al., 2007, Chen et al., 2008). In situations where the gauge-based data appear to show unusually high or low values, other satellite, modeled, and surface products are used to augment the gauge readings (Chen and Xie, 2008). CPC Morphing (CMORPH) data based on a microwave satellite sensor and infrared images is the satellite product used to supplement the gauge data (Joyce et al., 2004). The National Environmental Prediction Center's (NCEP) General Forecast System (GFS) is also used to supplement the gauge

data. Because the study area for this thesis is primarily in the tropics, CMORPH is likely the primary supplement, because previous work has found that CMORPH performs well over the tropics and sub-tropics (Ebert et al., 2007). Historical records from nearby stations are used to corroborate records in addition to CMORPH and the GFS model (Chen and Xie, 2008). CPC comes on a daily temporal scale and was summed to monthly values for this study. The data are available from 1979 to the present at a 0.5° by 0.5° spatial resolution.

2.1.3. Interpolated Station Precipitation

The Climatic Research Unit Timeseries Version 4.01 (CRU) is a gridded product released by the University of East Anglia. Comprised of station data from 1000s of rain gauge stations that are provided by the World Meteorological Organization WMO, the National Climatic Data Center, and numerous other national meteorological organizations, the product is not merged or blended with any other precipitation data and is based upon interpolated station data alone. Station coverage over southern Africa, particularly Namibia, is the caveat to a dataset that is only based on station observations. However, Zhang et al. (2013) found that when compared to the Global Precipitation Climatology Center and Global Precipitation Climatology Project (GPCP) datasets over southern Africa, an earlier iteration of the CRU dataset (CRU TS v3.1) was found to correlate well with the other precipitation datasets. In that study it was actually used as the baseline dataset for all of southern Africa. The dataset is provided at a monthly temporal resolution and did not require resampling. The data are available from 1979 to 2016 at a 0.5° by 0.5° spatial resolution.

2.1.4. Reanalysis Precipitation

European Centre for Medium-Range Weather Forecasts Reanalysis-Interim (ERA) is an atmospheric reanalysis that ingests global climate data into a numerical weather prediction (Dee et al., 2011). ERA-Interim is a commonly used global reanalysis dataset released by the European Centre for Medium-Range Weather Forecasts. It has been used to look at precipitation over river basins in North and West Africa and a comparison of different precipitation datasets over Uganda (Maidment et al., 2013, Thiemig et al., 2013). ERA-Interim was chosen based on evidence that suggested ERA-Interim to perform better than other global reanalysis products, such as the Modern-Era Retrospective analysis for Research and Applications in Africa (Tesfaye et al., 2017). The data were originally provided as a daily precipitation average for the month, and are from 1979 to the present at a 0.75° by 0.75° spatial resolution.

2.2. Teleconnections

2.2.1. Indian Ocean Dipole/Dipole Mode Index

The Dipole Mode Index is related to the IOD anomaly (Saji and Yamagata, 2003). The IOD index records the relationship between SST anomalies in the western Indian Ocean (50°E - 70°E and 10°S - 10°N) and the southeastern Indian Ocean (90°E - 110°E and 10°S - 0°N). The data are available from 1870 to the present and are derived from the Hadley Centre Global Sea Ice and Sea Surface Temperature (HadISST) dataset. When the IOD is in its positive mode, SST in the western Indian Ocean will be anomalously high, while SST in the southeastern Indian Ocean is anomalously low. Conversely, when the IOD is in its negative mode, SST in the western Indian Ocean will

be anomalously low, while SST in the southeastern Indian Ocean is anomalously high. The IOD oscillates on an annual to biennial timescale. The IOD has been found to drive climatic variability in East Africa and could potentially play a role in climatic variability over Namibia (Marchant et al., 2007).

2.2.2. Southern Oscillation Index

The SOI utilizes standardized sea level pressures (SLP) from Darwin and Tahiti. The CPC SOI data used here are available from 1951 to the present. A negative SOI value corresponds to low air pressure around Tahiti and high air pressure around Darwin, Australia. The SOI is the atmospheric aspect of ENSO, which takes in to account both SST (El Niño) and SLP (Southern Oscillation). SOI has a timescale that varies from two to seven years. The index was included because multiple studies have found a relationship between the SOI and precipitation over southern Africa (Lindesay, 1988, Lindesay and Vogel, 1990). The assumption was that the results for the SOI should align with past findings and the El Niño results (because it often acts as a coupled system).

2.2.3. Tropical Southern Atlantic Index

Tropical SST anomalies in the southern Atlantic Ocean are used as inputs for the Tropical Southern Atlantic Index (TSA) (Enfield et al., 1999). The SST anomalies are bounded by 10°E - 30°W and 0°S - 20°S. The data are available from 1948 to the present. The Hadley Centre Global Sea Ice and Sea Surface Temperature and NOAA Optimum Interpolation 1°×1° datasets were used to create the index. It is only based on one region's SST, not a dipole relationship between two separate locations. The

timescale varies depending on season, with changes approximately eight to twelve years for the austral summer/fall and changes approximately two years for the austral winter/spring. With a bounding box that ends just north of the Namibian coastline, the TSA has the potential to directly impact precipitation over Namibia.

2.2.4. North Atlantic Oscillation

The North Atlantic Oscillation (NAO) is an index that utilizes normalized pressure measurements from stations in Iceland and Portugal (Hurrell, 1995). The NAO index used here is derived by the NOAA Climate Prediction Center. The data are available from 1950 to the present. The NAO is known to have a direct effect on climate in the northern Hemisphere (Jones et al., 1997). For this study, NAO was chosen to represent atmospheric variability over the North Atlantic as a metric for measuring whether conditions in the North Atlantic drive precipitation over Namibia.

2.2.5. Pacific Decadal Oscillation

The first principal component of SST anomalies from the global SST average in the Pacific Ocean north of 20°N is defined as the Pacific Decadal Oscillation (PDO) (Zhang et al., 1997). The PDO was calculated using the UKMO Historical SST dataset from 1900 to 1981, the Reynold's Optimally Interpolated SST (V1) from 1982 to 2001, and the OI SST Version 2 (V2) from 2002 to the present. The PDO dataset used here is available from 1900 to the present. The PDO tends to oscillate over a twenty to thirty year period, with two complete oscillations thought to have occurred in the 20th century. The PDO was originally identified as it relates to salmon production in the northern Pacific Ocean (Mantua et al., 1997). Because the Pacific Ocean is known to play an

important role in African climate, and the PDO is an ENSO-like pattern over a longer time scale, it was thought that the PDO should be included to identify any potential teleconnections that might connect Namibian precipitation with the Pacific SSTs.

2.2.6. El Niño

As has already been discussed, El Niño is known to play an important role in precipitation across Africa, particularly in southern Africa (Hoell et al., 2017). Because El Niño is the SST component of ENSO and past research has found significant relationships between ENSO and southern African precipitation, it was important to include the numerous measures of El Niño. With numerous indices based upon SSTs in different sectors of the Pacific Ocean, each index reflects a different aspect of Pacific SST. All of the following datasets, with the exception of the Trans-Niño Index (TNI), are derived from the NOAA Extended Reconstructed SST V5 and are available from 1950 to the present. TNI is derived from the HadISST1.1 dataset from 1948 to November 1981, and latest OI SST from December 1981 to the present. TNI is available from 1948 to the present. The El Niño indices have a similar timescale to SOI, with changes every two to seven years.

2.2.6.1. Oceanic Niño Index

The Oceanic Niño Index (ONI) is based on a three month running average of SST anomalies in the central tropical Pacific Ocean (120°W - 170°W and 5°S - 5°N). The index is one of the three most commonly used metrics to decide when an El Niño (or La Niña) event is occurring (Trenberth, 2016). For this reason, ONI was one of the indices included in this study. Unlike the indices based in the northern Hemisphere, such

as the NAO and PDO, it was expected that there would be a significant correlation between precipitation over Namibia and the index.

2.2.6.2. Niño Indices: (Niño 1+2, Niño 3, Niño 3.4, and Niño 4)

Based on SSTs in a small region off the coast of Peru (80°W - 90°W and 0°S - 10°S), the Niño 1+2 Index is the most variable of the numerous Niño indices, likely due to its relatively small geographic area (Trenberth, 2016).

The Niño 3 Index is based on SST in the eastern Pacific (90°W - 150°W and 5°N - 5°S), and was originally used as the primary index to measure the phase and strength of the El Niño cycle. However, after further exploring what portion of the Pacific Ocean best represents ENSO's ocean-atmosphere coupling, Trenberth (1997) defined the central and central-western tropical Pacific Ocean as the region that best defines ENSO. This new Niño 3.4 region is bounded in the same area as the ONI (120°W - 170°W and 5°S - 5°N), and the Niño 3.4 Index is widely considered to be one of the most if not the most important index for discerning El Niño cycles. The region used for Niño 3.4 and ONI corresponds with the area that Trenberth (1997) found to be most important for ocean-atmosphere interactions.

Niño 4 stretches from the central Pacific Ocean westward, into the western Central Pacific Ocean (160°E - 150°W and 5°S - 5°N). It is stated in Trenberth (2016) that Niño 4 generally has the least variability of the numerous Niño indices.

2.2.6.3. Trans-Niño Index

Utilizing anomalies from Niño 1+2 and Niño 4, TNI was developed to describe the difference in SSTs on the eastern and western ends of the tropical Pacific Ocean. The

index was thought to be a necessary inclusion in the El Niño event identification process by Trenberth and Stepaniak (2001). TNI provides an indication of whether the oscillation of tropical Pacific SSTs is connected with the study region.

3. METHODS

3.1. Regridding

To quantify how the different products compare to TRMM, a common spatial resolution is necessary. The different spatial scales were regridded to the coarsest spatial resolution of all products—ERA's 0.75° by 0.75°. Three of the four datasets (CPC, CRU, and TRMM) were extracted to an exact domain of 16° - 30° South and 11° - 22° East. The ERA-Interim grid did not align exactly with the target domain and thus extends out to 15.375° - 30.375° South and 10.125° - 22.875° East.

The regridding method used is a First Order Conservative Area remapping that was developed by Jones (1999). It incorporates all finer grid cells from the original grid in to the coarse grid cells of the target grid. This method is an improvement over the nearest-neighbor or bilinear remapping methods, which both have the potential to not incorporate all of the finer grid cells into the larger grid cells of the target grid. The First-Order regridding method has been previously used for the CMORPH data product to remap grid cells to a coarser resolution, as well as for other precipitation studies (Belo-Pereira et al., 2011, Nikulin et al., 2012, Contractor et al., 2015).

3.2. Dataset Comparisons

With only sixteen to seventeen years of data, the TRMM 3G68 Land product does not have a long enough record to establish a long-term precipitation climatology for Namibia. Because of that, TRMM cannot be used to determine the climatological drivers of precipitation variability in Namibia. However, with an original spatial resolution of

0.1° by 0.1°, it offers high-resolution precipitation estimates for Namibia. The Spearman correlation coefficient, root mean squared error (RMSE), mean error (ME), and mean absolute error (MAE) are used to calculate which dataset compares best with TRMM.

3.2.1. Spatial Analysis

Four metrics were used to identify which dataset best compares with TRMM after all four products were regridded to a common resolution. Because precipitation data do not generally follow a normal distribution (especially in a semi-arid region with high precipitation variability) the Spearman Rank correlation coefficient was used to identify which datasets correlate best with TRMM. RMSE is a common metric to calculate the magnitude of difference between two datasets. Because the errors are squared, all values are positive. MAE is a similar error metric that does not square the error, but instead takes the absolute value. Consequently, all MAE values are also positive. The last error metric used here is a ME calculation. Unlike the other two error metrics, ME does have both negative and positive values. This allows for an interpretation of whether there is an overestimation or underestimation against the baseline. However, when the ME values are averaged, there is the potential caveat that negative and positive values will cancel one another out and show little error where that is not the case. Nonetheless, the metric can be useful when utilized in consortium with the other metrics. An independent t-test is utilized to determine whether the ME results are statistically significant.

3.2.2. Annual/Monthly Climatologies and Trend Analysis

To assess the temporal correspondence of the three products with TRMM, all datasets were averaged across Namibia to create single monthly time series for each dataset. However, averaging precipitation across an area characterized by high spatial variability may not result in a meaningful spatial average. Therefore, to further assess the temporal correspondence of the three products, three sub-regions of similar sizes located throughout Namibia were selected. The chosen regions are river basins, with precipitation averaged across the entire river basin. Approximately 15,000 square kilometers in size, the basins were selected to best capture the localized precipitation patterns in different parts of Namibia. Time series of precipitation from January, 1998 to September, 2014 were created at the monthly and annual time scale, with correlation coefficients calculated for each dataset against the TRMM baseline. The same metrics used in the spatial analysis, Spearman, RMSE, MAE, and ME are also used on the country-wide and basin time series. Average monthly totals for all months of the year were calculated.

For annual trends, a linear least-squared regression trend analysis was used. To capture potential non-parametric trends in the monthly data, the Mann-Kendall Test was applied, with the Theil-Sen estimator used to calculate the slope of any statistically significant, non-parametric trends. Trends were calculated for all twelve months and at an annual time scale from January, 1998 to September, 2014.

3.3. Namibia's Precipitation Climatology and Long-term Trends

Once the "best" dataset relative to TRMM is identified, it will be used to establish a comprehensive, long-term precipitation climatology, and for trend analysis for Namibia's precipitation. In addition to yearly and monthly analyses, Namibia's rainy season will be assessed, with the rainy season period defined based upon the results of the month analyses.

3.4. Namibia's Precipitation Drivers

The ultimate goal of this thesis is to determine what causes precipitation variability in Namibia. To identify the drivers of precipitation variability, numerous climate indices representing global teleconnections are used.

3.4.1. Drivers of Grid Cell-Level Precipitation Variability

A Pearson correlation was performed between all ten of the aforementioned indices and each grid cell of the ERA-Interim precipitation product over Namibia. The correlations were performed at the monthly, yearly, and rainy season time scales. To address the issue of multiple-comparison effects, a Bonferroni adjustment is applied to the p-value of 0.05.

3.4.2. Drivers of Major Modes of Precipitation Variability

PCA is a useful technique that identifies the dominant modes of variability within a dataset by reducing the dimensions of the dataset. Comparisons that were not possible with 171 variables are now possible when only a couple of the dominant PCs are used. Utilizing the first two PCs —the components that account for most of the variance—are then correlated to the climate indices to determine their relationship.

Because most of the variance is accounted for in the first and second principal components, they are the only components evaluated in this study. The principal components were correlated against all ten of the climate indices once again at the yearly, monthly, and rainy season time periods.

4. RESULTS

4.1. Precipitation Comparison

Due to Namibia's sparse gauge network, the satellite observations from TRMM's PR sensor were determined to be the best product to evaluate Namibia's precipitation variability. However, due to the short timeframe that TRMM is available, from 1998 to 2014, another product with increased temporal coverage was needed. However, because TRMM was still considered the best product for studying precipitation over Namibia, the TRMM product was used as a baseline dataset for other products to be compared against.

Figure 4.1. Original (left) and regridded (right) annual precipitation climatology for 1998 to 2013 using the TRMM dataset.

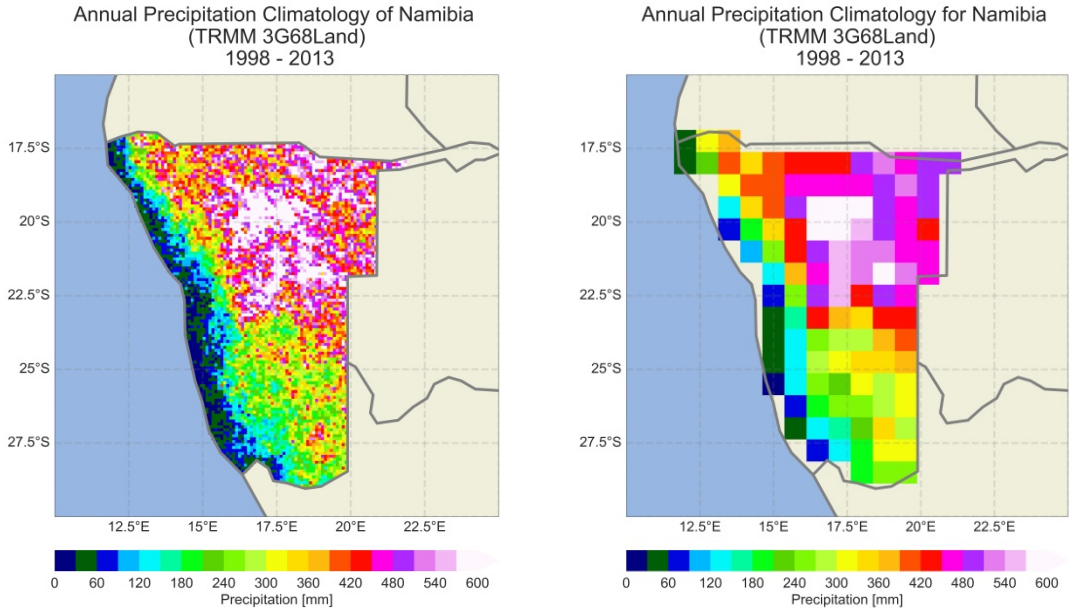

ERA, CPC, and CRU were chosen to be compared against the TRMM baseline. Climatologies for both the original and regridded TRMM product are shown above (Figure 4.1). To provide additional context, boxplots showing the annual cycle are also shown for both the original and regridded TRMM products (Figure 4.2). The boxplots show that only slight shifts are evident in the TRMM product after being regridded from 0.1° by 0.1° to 0.75° by 0.75°.

4.1.1. Spatial Analysis

To find the long-term dataset that best captures precipitation variability in Namibia, the Spearman, RMSE, MAE, and ME metrics are calculated on the 0.75° by 0.75° regridded precipitation products over the 1998 – 2014 period. The metrics are calculated against TRMM, which is considered to be the baseline product. Specific thresholds were chosen for each error metric to identify which dataset agrees most closely with TRMM across Namibia. The RMSE and ME thresholds were chosen as one deviation of the 171 gridcells in each of the three datasets. The number of grid cells with RMSE values below the threshold were recorded (Table 4.1). Dry season months, May through September, were not included due to low precipitation.

RMSE results for the three datasets suggest that the errors for CRU are lower for all rainy season months and at the annual timescale. For example, the RMSE results for January suggest that CRU errors are less compared to ERA and CPC (Figure 4.3).

CPC has higher error values along the coastline, a region of little rainfall, as well as high RMSE values inland where greater precipitation amounts are usually recorded. With only 19 of the 171 cells passing the RMSE threshold, CPC has few cells with low

Figure 4.2 Original (top) and regridded (bottom) annual precipitation cycle for 1998 to 2014 using the TRMM dataset. The 1st and 3rd quartiles are shown by the edges of the boxes, the whiskers represent the minimum and maximum temperatures, and the medians are plotted as horizontal lines with the boxes. The means are represented by the dots.

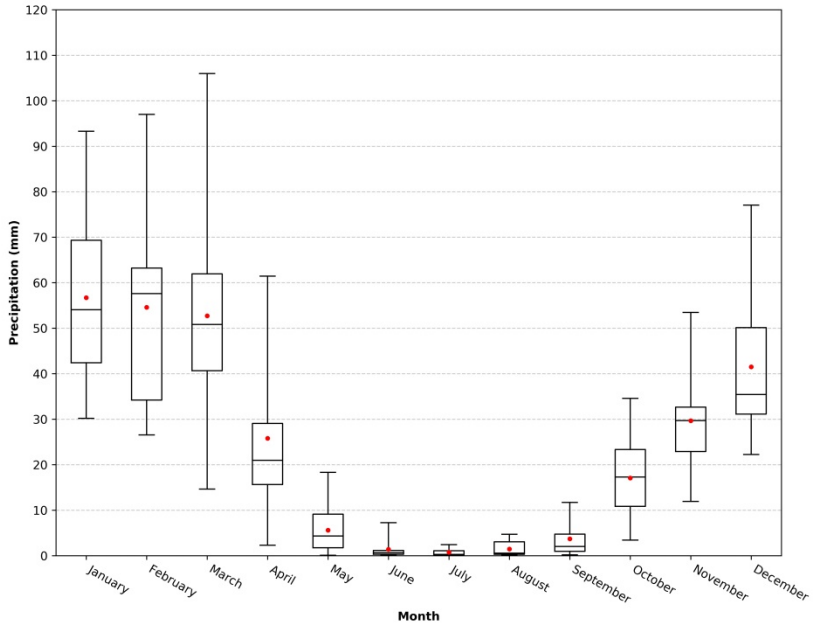

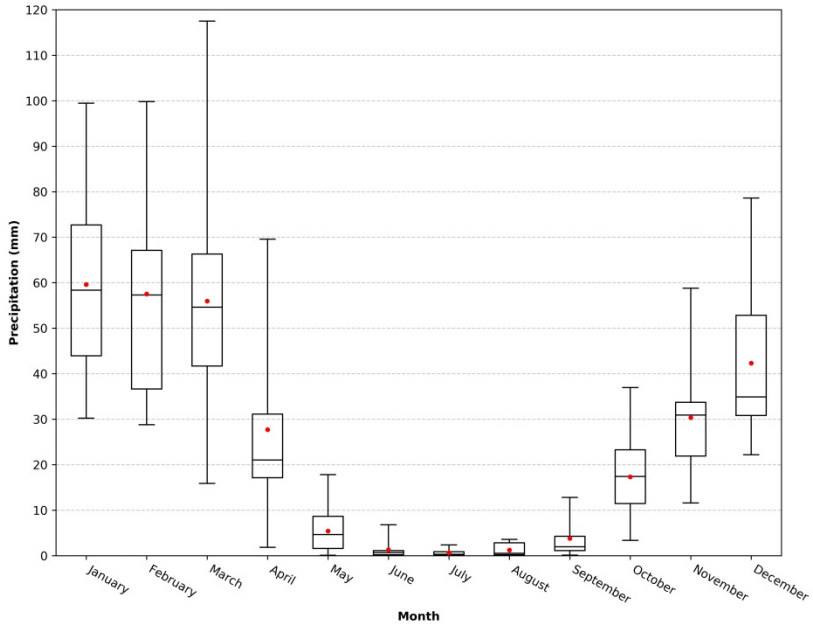

Table 4.1. Total number of grid cells per dataset with values 1 standard deviation below the RMSE average.

	RMSE							
	Jan	Feb	Mar	Apr	Oct	Nov	Dec	Annual
ERA	27	24	28	13	27	28	28	31
CPC	19	31	27	20	29	25	25	20
CRU	34	36	31	27	34	35	31	31

errors. The ERA dataset compares well to the baseline along the coastal region, with low RMSE values over the Namib Desert. Compared to CPC, ERA has over 40% more cells (27 versus 19) with RMSE values below the threshold. However, with 34 of

Figure 4.3. January RMSE precipitation comparison in mm for ERA (left), CPC (center), and CRU (right) against TRMM 3G68Land from 1998 to 2014.

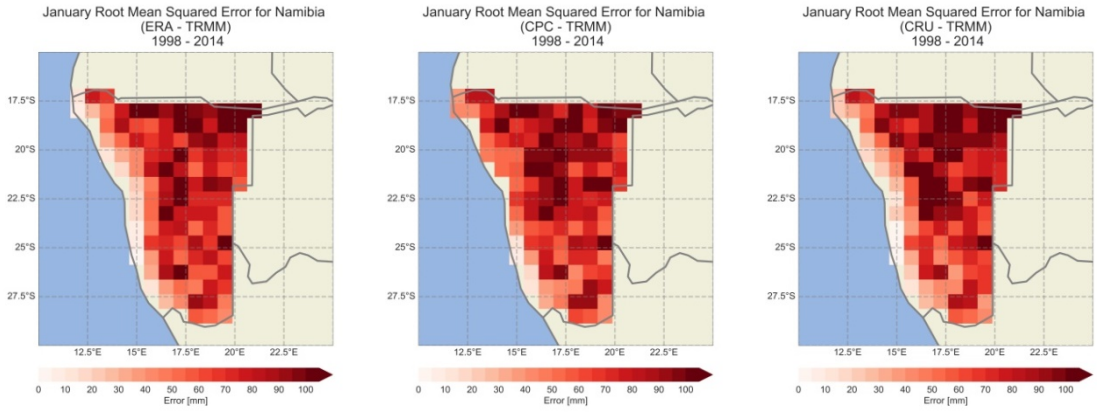

the 171 cells below the threshold, CRU still provides the most cells with low errors in January. There were over 25% more cells below the threshold for CRU than for ERA.

While January is a representative example of when CRU proved to have a significantly greater number of cells below the 1 standard deviation threshold, at the annual time scale CRU agrees with TRMM equally as well as ERA (Figure 4.4).

Figure 4.4. Annual RMSE precipitation comparison in mm for ERA (left), CPC (center), and CRU (right) against TRMM 3G68Land from 1998 to 2013.

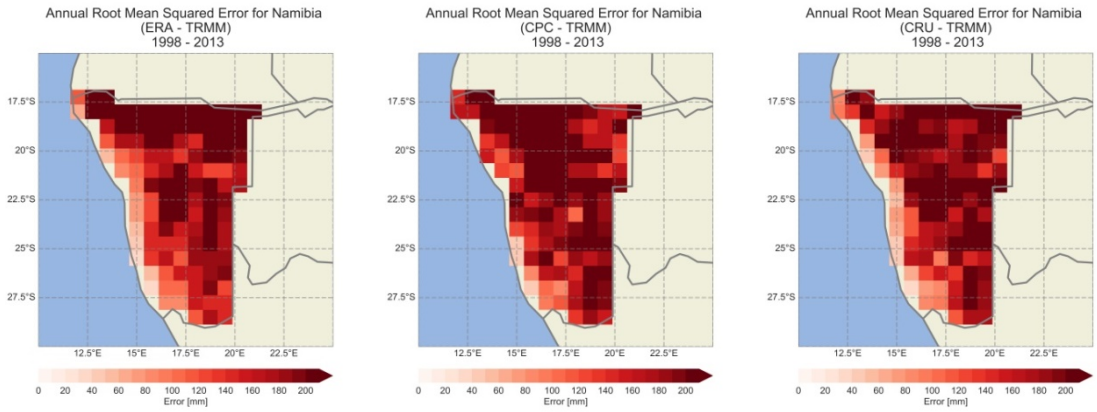

While CPC has considerably fewer values below the threshold than the other two datasets, ERA and CRU are tied with exactly 31 cells each below the threshold. The highest RMSE results from the ERA dataset stretch along the northern border with Angola up to the coastline, where the RMSE values once again decrease. In the southern half of the country, high RMSE values appear patchy, though with a definite decrease compared to the northern band.

The RMSE results for CRU show a distinctly different spatial pattern. While a narrow band of high RMSE stretches across the north of the country, the highest errors are also predominant through the central and southern portions of the country. The coastal region has predominantly low errors, with an increase only occurring farther inland.

MAEs for all the evaluated time periods show that the CRU dataset has the highest number of cells below the threshold for all time periods except March and April (Table 4.2). The MAE calculated for January provides a best case for the errors between CRU and TRMM (Figure 4.5). There are 35 cells with MAE below the threshold, 6 more than ERA.

Table 4.2. Total number of grid cells per dataset with values 1 standard deviation below the MAE average.

	MAE							
	Jan	Feb	Mar	Apr	Oct	Nov	Dec	Annual
ERA	29	25	27	25	31	33	33	28
CPC	24	31	34	33	34	27	24	20
CRU	35	33	28	33	37	37	34	30

March and April are outliers in the MAE results when CPC has the most cells with MAE below the threshold (34 to 28 cells), an increase in cells of just over 20%, in

March. In April, the two datasets have an equal number of 33 cells below the threshold. The CRU dataset has the lowest errors based on MAE while the MAE results for the ERA dataset suggest that the errors are relatively high.

Figure 4.5. January MAE precipitation comparison in mm for ERA (left), CPC (center), and CRU (right) against TRMM 3G68Land from 1998 to 2013.

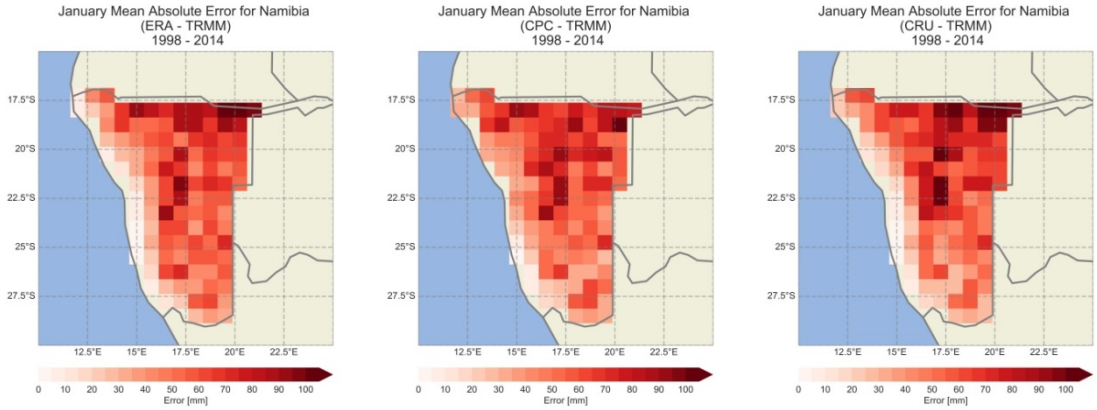

Based on the number of statistically significant ($p<0.05$) Spearman correlations, five of the eight timeframes indicate the best agreement between ERA and TRMM (Table 4.3). The November results show that ERA has 49 cells with statistically significant positive correlations with the TRMM baseline (out of the 171 total grid cells). CPC comes in second for November, with only 10 cells. The few CPC cells that do have statistically significant positive correlations are scattered across northern Namibia (Figure 4.6). The ERA cells that correlate stretch throughout most of Namibia, with statistically significant positive correlations along the dry coastline and the wet interior. There are three months when CPC saw more grid cells with positive correlations than

ERA. The February Spearman analysis shows CPC with 65 significant correlations while the ERA dataset had only 57.

Table 4.3. Total number of grid cells with statistically significant Spearman Rank correlation coefficients.

	SPEARMAN							
	Jan	Feb	Mar	Apr	Oct	Nov	Dec	Annual
ERA	49	57	36	100	54	49	23	69
CPC	32	65	38	87	60	10	20	52
CRU	32	45	23	63	19	8	19	43

Figure 4.6. November Spearman rank correlation comparison for ERA (left), CPC (center), and CRU (right) against TRMM 3G68Land from 1998 to 2013.

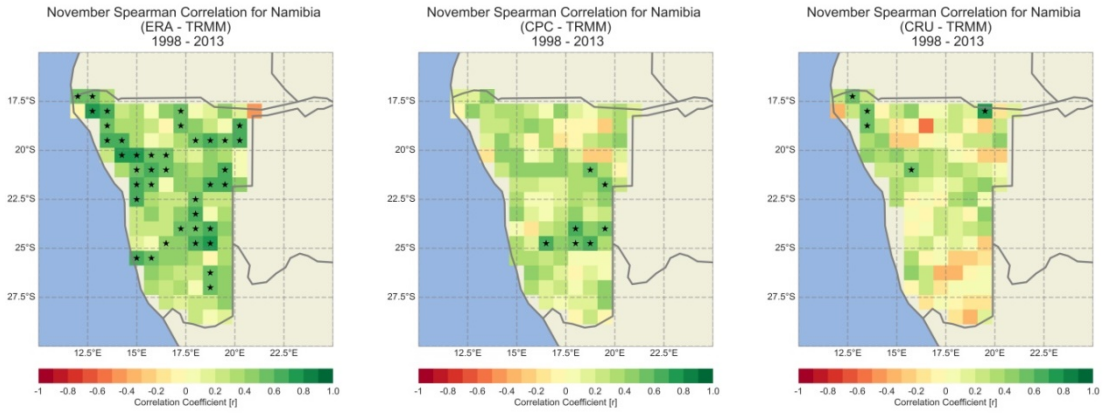

Based on statistically significant ME, datasets with fewer cells with significantly different errors are considered to be better. This method provided a less conclusive result than RMSE, MAE, or the Spearman correlation (Table 4.4). ERA had the fewest significant cells for October, December, and at an annual time period, however CRU had the fewest significant cells for January through March. CPC had the fewest significant cells for the remaining months of April and November. ERA is shown to have comparatively the fewest significant errors in October and annually. The annual results suggest that ERA severely underestimates precipitation in northern Namibia while there is a better relationship in central and southern Namibia (Figure 4.7).

Figure 4.7. Annual ME Comparison in mm for ERA (left), CPC (center), and CRU (right) against TRMM 3G68Land from 1998 to 2013.

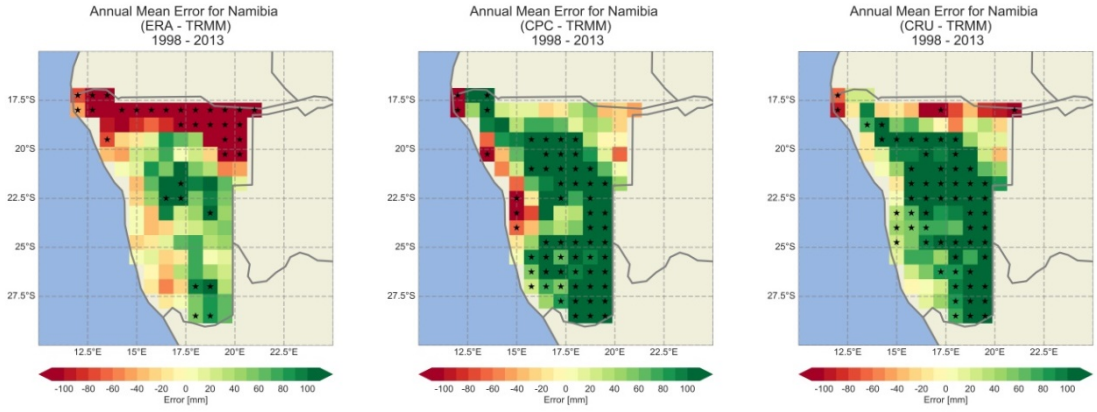

This result is the opposite of the ME for CPC and CRU. Both datasets have a greater number of statistically significant errors. The errors suggest a strong overestimate of the precipitation in central and southern Namibia, while the errors in

Table 4.4. Total number of grid cells with statistically significant ME.

	ME							
	Jan	Feb	Mar	Apr	Oct	Nov	Dec	Annual
ERA	33	23	20	9	8	28	33	57
CPC	32	12	30	8	22	18	37	80
CRU	26	7	14	14	28	29	54	80

Figure 4.8. March ME comparison in mm for ERA (left), CPC (center), and CRU (right) against TRMM 3G68Land from 1998 to 2014.

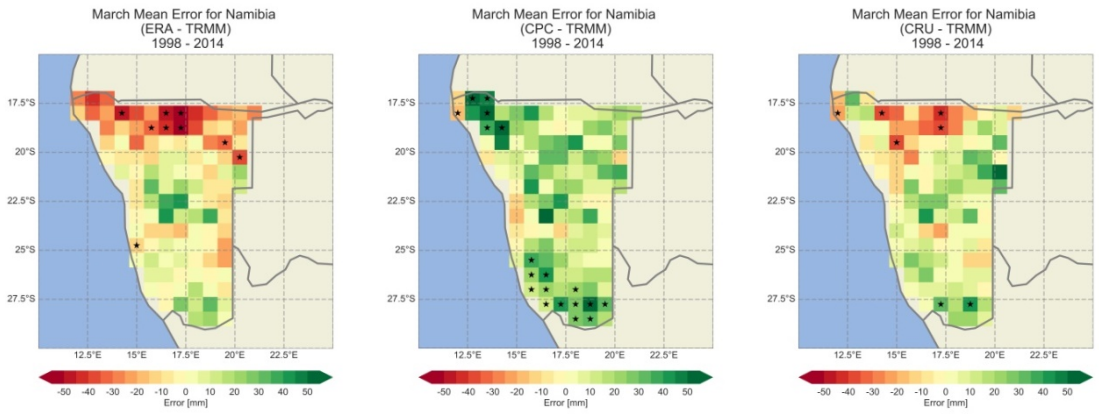

northern Namibia are better for both CPC and CRU. The ME in the month of March shows CRU with fewer significant errors than CPC or ERA (Figure 4.8). CRU has 14 cells with significant errors scattered across Namibia, CPC and ERA show and an

overestimation and an underestimation of precipitation with 30 cells and 20 significant ME cells, respectively.

Figure 4.9. Map of drainage basins across Namibia (evaluated basins highlighted with red boundaries).

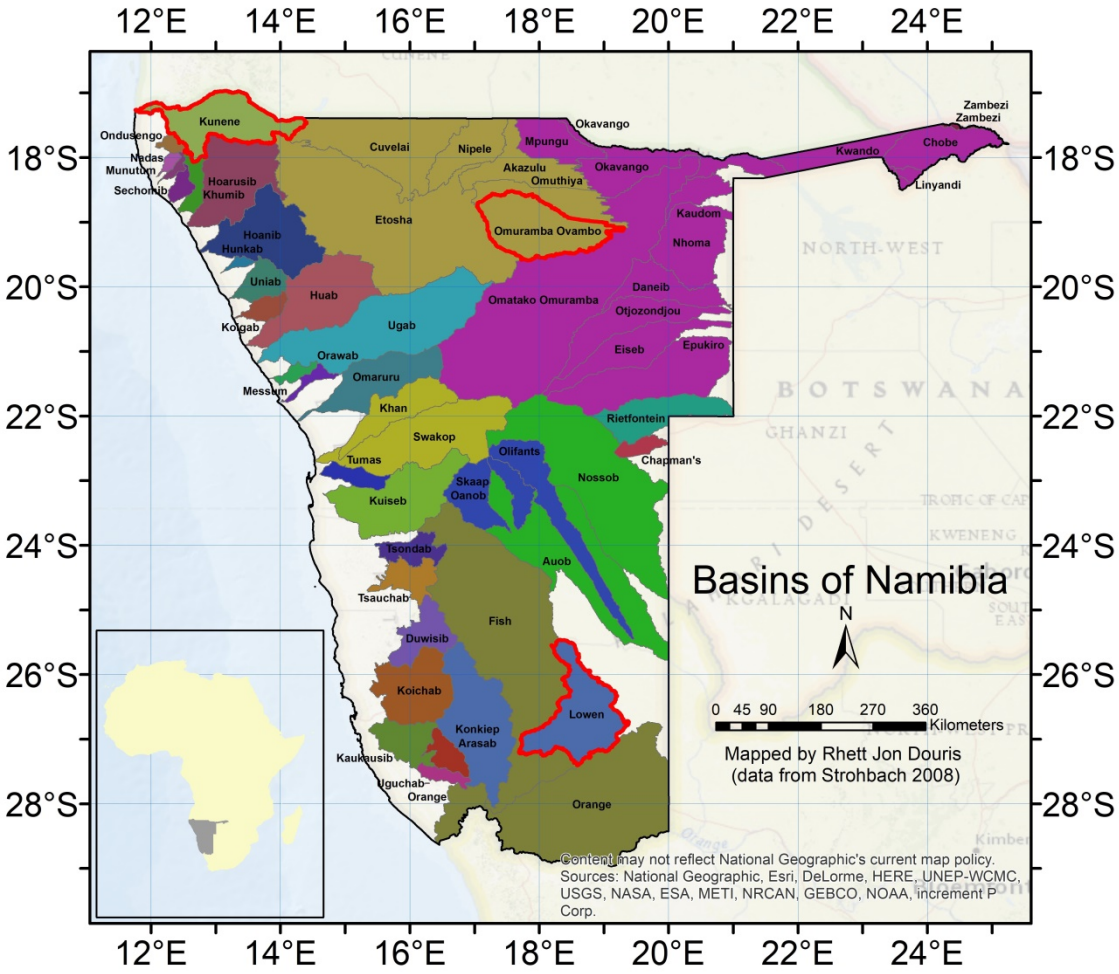

4.1.2. Temporal Analysis

With a temporally variable precipitation regime, evaluating precipitation across Namibia is a challenge. To assess the products' agreement with the TRMM baseline over time, a country-wide spatial average was calculated. Because this removes the

spatial variability of Namibian precipitation, with high and low precipitation regions potentially averaging out one another, separate regions were necessary. The country-wide and basin analyses use the same metrics as in the spatial analysis. RMSE, MAE, ME, and Spearman correlation coefficients are calculated. A Pearson's correlation was also performed on the annual time series against the TRMM baseline.

To better understand the temporal and spatial precipitation patterns across Namibia, three drainage basins of roughly equal size (approximately 15,000 square kilometers) were evaluated. To capture as much of the spatial variation of Namibia as possible, the three basins selected are located in different parts of Namibia (Figure 4.9) (Strohbach, 2008). Precipitation across each basin was averaged at a monthly timescale.

Figure 4.10. Country-wide annual time series for ERA (orange), CPC (blue), CRU (green) and TRMM (red) with precipitation levels given in mm and the Pearson correlation coefficients calculated against TRMM.

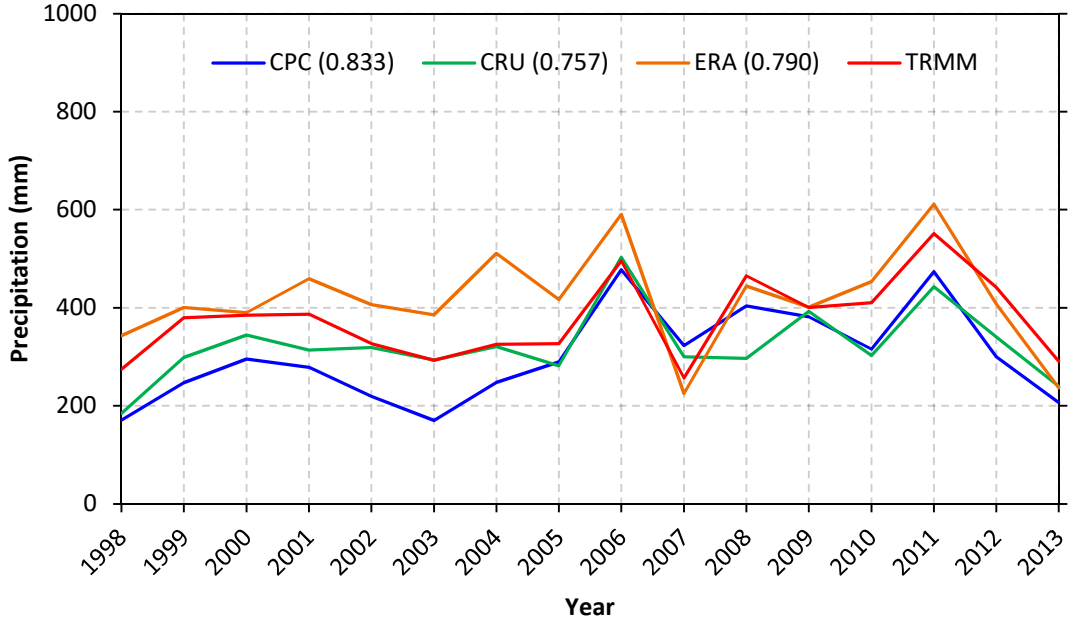

The Kunene Basin is located in the farthest corner of northwestern Namibia. The basin borders (and slightly extends into) the Namib Desert along the coastline. The Omuramba Ovambo Basin is an interior basin located in northeastern Namibia. Of the three basins, it is located in a region that receives the highest levels of annual precipitation. The Löwen basin is at the southernmost tip of Namibia. While the basin is situated towards the interior of southern Namibia, the tapering of the country means that it is closer to the coastline than the Omuramba Ovambo Basin.

Figure 4.11. Kunene Basin annual time series for ERA (orange), CPC (blue), CRU (green) and TRMM (red) with precipitation levels given in mm and the Pearson correlation coefficients calculated against TRMM.

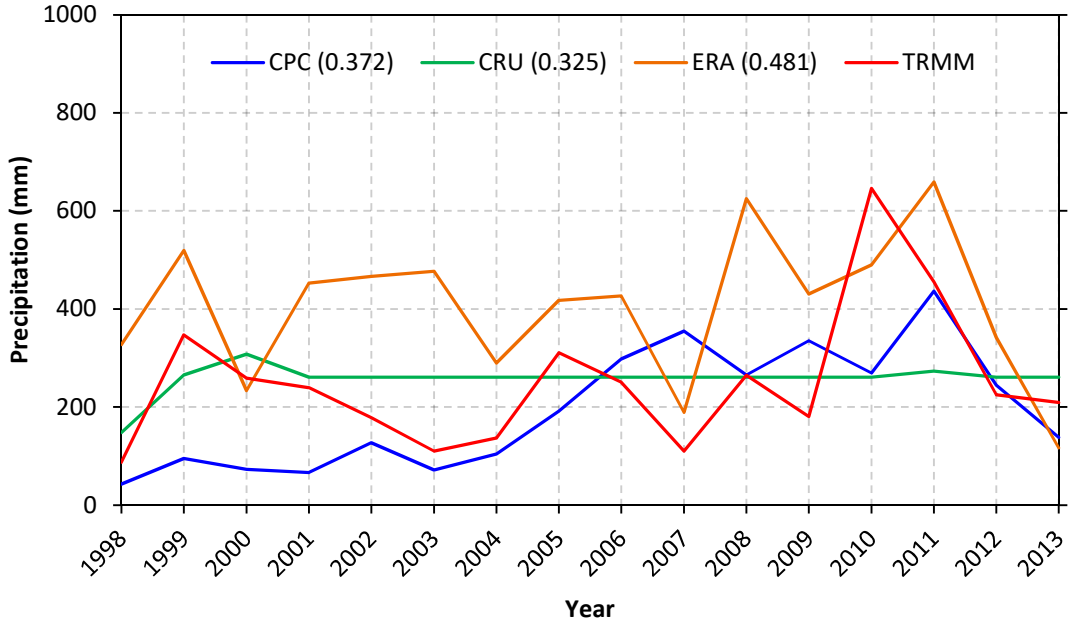

The country-wide time series comparison for Namibia suggests a different result from the three basin analyses. CPC has the highest correlation value at 0.83 (Figure 4.10). The ERA and CRU correlation values are 0.79 and 0.76, respectively. ERA

overestimates precipitation from 2001 to 2006. While CPC underestimates precipitation from 1999 to 2004, the underestimate is smaller than the ERA overestimate. CRU underestimates precipitation in the early 2000s and 2010s.

In the Kunene Basin from 1998–2013 none of the precipitation products were correlated with TRMM (Figure 4.11). This temporal analysis revealed that the original CRU grid values are in-filled with identical values for multiple years, perhaps owing to missing input data. While this pattern was only evident in the Kunene Basin, it is unknown how many additional grid cells across Namibia were also filled with multi-year averages.

Figure 4.12. Omuramba Ovambo Basin annual time series for ERA (orange), CPC (blue), CRU (green) and TRMM (red) with precipitation levels given in mm and the Pearson correlation coefficients calculated against TRMM.

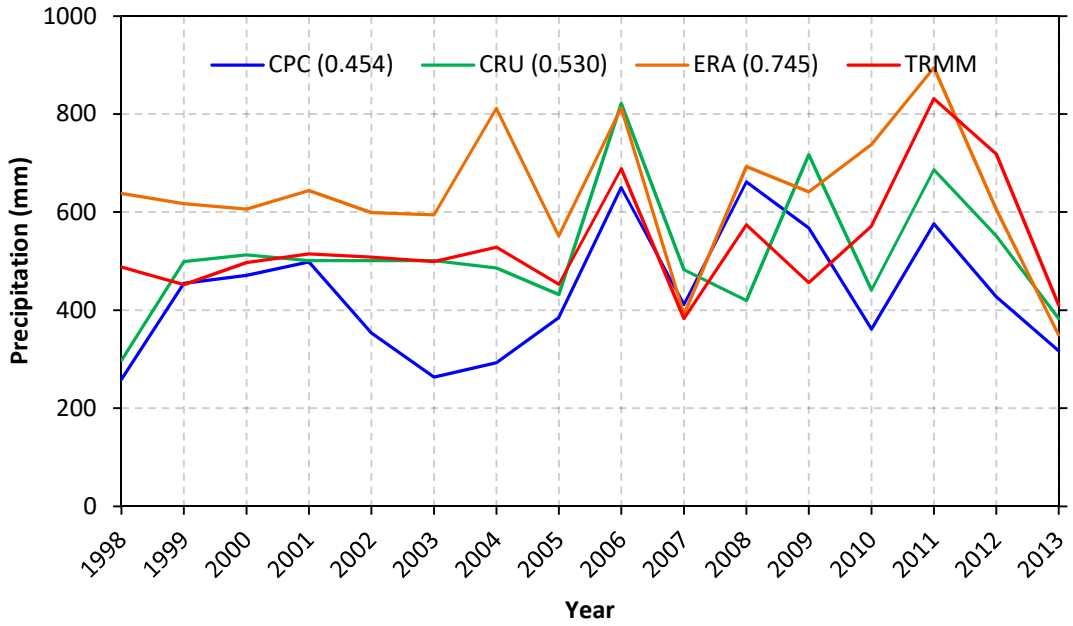

The correlation between ERA and TRMM for the Omuramba Ovambo Basin is 0.75 (Figure 4.12), while the correlation value between CRU and TRMM is only 0.53. The CPC correlation does not correlate with TRMM. The annual CRU results are unusual, because they appear to be out of phase with the TRMM baseline for certain time periods. ERA and TRMM show an increase in precipitation in both 2008 and 2010, with a decrease in 2009.

However, CRU shows a precipitation decrease in 2008 and 2010, with an increase in 2009. CPC generally matches TRMM in 2008 and 2009, but then decreases in 2010, similar in pattern to the CRU value for 2010.

Figure 4.13. Löwen Basin annual time series for ERA (orange), CPC (blue), CRU (green) and TRMM (red) with precipitation levels given in mm and the Pearson correlation coefficients calculated against TRMM.

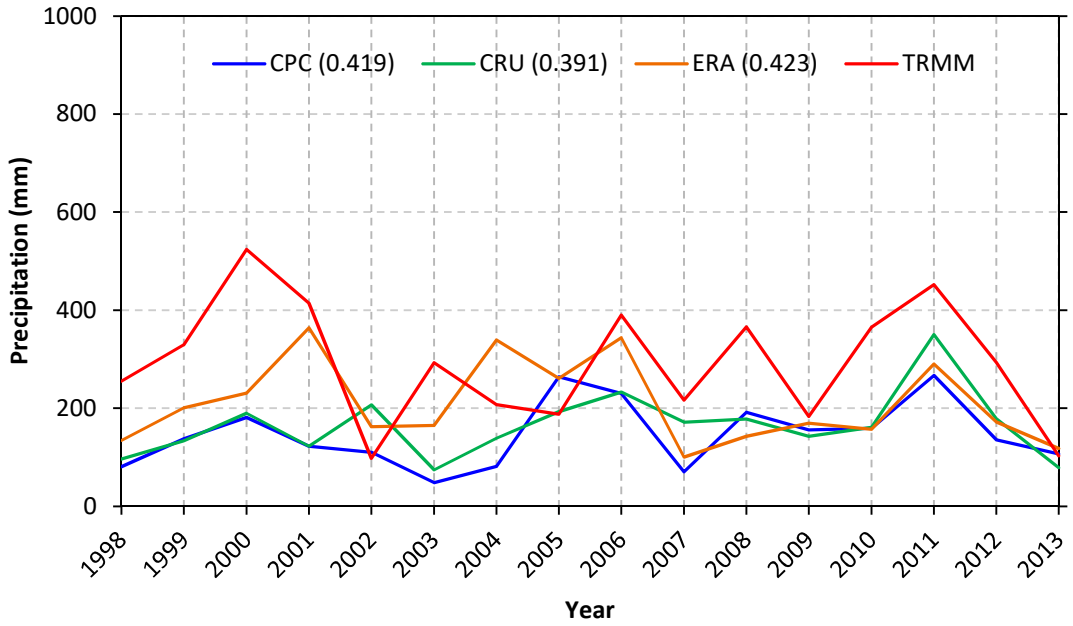

Table 4.5. Spearman coefficients, RMSE, MAE, and ME statistics for ERA, CPC, and CRU against the TRMM baseline with data for all of Namibia. RMSE, MAE, and ME statistics are given in mm (bold values denote significance at the p<0.05 level).

		Namibia							
		Jan	Feb	Mar	Apr	Oct	Nov	Dec	Annual
RMSE	ERA	24.58	29.51	23.42	11.09	10.34	12.86	21.92	74.01
	CPC	25.08	18.59	26.94	12.92	12.09	21.97	24.64	91.26
	CRU	29.12	21.96	23.26	14.94	15.38	16.30	21.77	75.14
ME	ERA	-11.60	-16.78	-9.55	5.17	7.23	-6.74	-8.37	-41.90
	CPC	5.46	8.85	**18.90**	9.53	**10.10**	6.09	10.82	**75.66**
	CRU	0.10	-2.23	1.38	9.18	**11.32**	**12.41**	10.31	52.13
MAE	ERA	17.33	25.00	16.68	8.91	9.07	10.87	18.17	59.60
	CPC	18.87	14.59	23.11	11.15	10.20	16.81	19.48	83.86
	CRU	18.83	19.01	20.80	10.72	13.14	12.81	11.81	58.57
SPEARMAN	ERA	**0.82**	**0.79**	**0.50**	**0.86**	**0.68**	**0.70**	**0.61**	**0.75**
	CPC	**0.84**	**0.83**	**0.61**	**0.91**	**0.66**	0.41	**0.54**	**0.74**
	CRU	**0.56**	**0.72**	0.46	**0.90**	0.40	**0.53**	0.48	**0.67**

The Löwen basin has the lowest correlation values of all three basins, with none of the datasets correlating to TRMM (Figure 4.13). All three datasets underestimate the TRMM baseline, particularly during the late 1990s and early 2000s. The error and correlation analyses, the temporal country-wide and basin values are calculated monthly

Table 4.6. Spearman coefficients, RMSE, MAE, and ME statistics for ERA, CPC, and CRU against the TRMM baseline with data for the Omuramba Ovambo basin. RMSE, MAE, and ME statistics are given in mm (bold values denote significance at the $p<0.05$ level).

		Omuramba Ovambo							
		Jan	Feb	Mar	Apr	Oct	Nov	Dec	Annual
RMSE	ERA	90.30	80.99	64.07	28.78	26.82	33.04	50.25	136.41
	CPC	88.58	68.34	56.02	28.68	25.23	63.22	63.91	161.66
	CRU	97.67	73.06	59.84	20.02	31.95	53.18	54.54	119.34
ME	ERA	-41.68	-17.61	-28.03	-7.90	12.39	-2.24	-19.24	**-100.88**
	CPC	-7.84	24.92	13.70	-1.16	12.47	21.19	23.61	**101.44**
	CRU	-20.77	-3.14	-17.51	-3.86	**16.96**	**26.95**	7.14	21.38
MAE	ERA	68.46	64.85	52.79	21.81	21.11	28.50	39.08	122.60
	CPC	65.41	52.54	37.69	15.54	20.19	51.36	49.53	130.25
	CRU	69.03	58.63	47.08	15.39	25.77	42.88	43.33	91.16
SPEARMAN	ERA	0.17	0.13	0.23	**0.64**	0.46	**0.58**	**0.64**	**0.72**
	CPC	0.11	**0.62**	0.46	**0.74**	**0.54**	0.06	0.29	0.38
	CRU	-0.31	0.47	-0.01	**0.64**	-0.02	0.13	0.41	0.44

from October to April. The dry season, from May through September, inclusive, was not evaluated due to little precipitation. A yearly analysis was also performed for all three datasets.

Table 4.7. Spearman coefficients, RMSE, MAE, and ME statistics for ERA, CPC, and CRU against the TRMM baseline with data for the Löwen basin. RMSE, MAE, and ME statistics are given in mm (bold values denote significance at the p<0.05 level).

		Löwen							
		Jan	Feb	Mar	Apr	Oct	Nov	Dec	Annual
RMSE	ERA	43.78	46.44	38.19	62.29	15.29	20.66	31.50	139.83
	CPC	52.98	52.46	42.95	64.02	16.34	23.56	45.03	182.21
	CRU	47.05	57.96	31.36	62.82	16.28	23.87	46.44	168.53
ME	ERA	19.53	10.27	6.44	22.84	3.35	5.52	16.67	**82.83**
	CPC	27.14	23.35	**21.90**	21.76	**8.79**	10.27	**25.08**	**145.93**
	CRU	21.27	11.55	8.42	29.49	6.68	6.27	**31.20**	**126.78**
MAE	ERA	33.29	34.97	32.19	31.66	11.00	12.53	22.42	118.53
	CPC	36.95	40.74	30.13	36.09	10.93	14.21	30.76	157.59
	CRU	30.17	47.65	26.88	33.85	11.17	16.50	32.47	141.08
SPEARMAN	ERA	0.48	0.38	0.24	**0.49**	0.33	0.39	0.33	0.45
	CPC	0.37	0.16	0.22	**0.50**	0.34	0.09	0.12	0.48
	CRU	**0.51**	0.07	0.32	**0.65**	0.15	-0.08	0.31	0.26

For the country-wide analysis, the RMSE, MAE, and ME results have the lowest errors with ERA, while the Spearman correlations show that ERA and CPC are tied with the most significant correlations. Based on the results, ERA is the best dataset country-wide (Table 4.5).

Table 4.8. Spearman coefficients, RMSE, MAE, and ME statistics for ERA, CPC, and CRU against the TRMM baseline with data for the Kunene basin. RMSE, MAE, and ME statistics are given in mm (bold values denote significance at the p<0.05 level).

		Kunene							
		Jan	Feb	Mar	Apr	Oct	Nov	Dec	Annual
RMSE	ERA	35.27	65.41	58.64	50.84	18.41	34.40	55.64	209.78
	CPC	50.02	31.63	63.36	55.01	14.50	44.39	41.62	154.59
	CRU	46.31	29.91	55.75	53.72	19.59	30.94	35.91	131.10
ME	ERA	-15.25	**-50.93**	-34.72	-2.52	-3.04	-16.64	-24.67	**-153.36**
	CPC	-6.35	-3.15	**36.81**	23.18	2.95	6.16	-4.74	55.79
	CRU	-14.26	-8.94	3.35	13.92	-3.64	5.13	-4.44	-7.36
MAE	ERA	28.69	53.85	48.32	31.04	11.73	25.32	43.31	187.64
	CPC	41.57	21.40	45.39	26.80	8.94	28.99	30.22	114.33
	CRU	38.55	25.94	40.12	29.08	12.48	23.54	29.85	94.99
SPEARMAN	ERA	**0.72**	**0.78**	**0.65**	0.47	0.46	**0.56**	0.48	**0.55**
	CPC	-0.02	**0.50**	0.30	**0.56**	0.48	0.33	0.25	0.31
	CRU	0.21	0.35	0.41	-0.22	0.26	0.49	-0.01	**0.60**

For the Omuramba Ovambo Basin, the RMSE, MAE, and ME results have the lowest errors with CPC, while the Spearman correlations show that ERA has the most significant correlations. Based on these results, CPC is the best dataset for the Omuramba Ovambo Basin (Table 4.6).

For the Löwen Basin, the RMSE, MAE, and ME results have the lowest errors with ERA, while the Spearman correlations show that CRU has the most significant correlations. Based on the results, ERA is the best dataset for the Löwen Basin (Table 4.7).

For the Kunene Basin, the RMSE, MAE, and ME results have the lowest errors with CRU, while the Spearman correlations show that ERA has the most significant correlations. Based on these results, CRU is the best dataset for the Kunene Basin (Table 4.8).

4.1.3. Precipitation Trends

Understanding and identifying changes in precipitation over time is a key aspect of this study. With a changing climate, there is the distinct potential for long-term precipitation trends to be evident. It is therefore important to assess whether CRU, ERA, and CPC exhibit similar trends as TRMM during their overlapping 1998–2013 period.

Annual linear least squares TRMM precipitation trends show a statistically significant increase along a narrow swath from northwest to southeast across Namibia (Figure 4.14). The other precipitation datasets do not capture the TRMM spatial trend pattern. Neither ERA nor CRU have any significant trends in Namibia. CPC has a statistically significant increase in precipitation along Namibia's northern and central coastline, which does not, however, align well with the baseline trends. Thus, the TRMM trend patterns are not captured in any of the other datasets.

Non-parametric trends (Mann Kendall test) were calculated for all twelve months for all datasets. It was expected that the data would not have a normal distribution at the

monthly scale, but instead would have a positive skew, due to the high number of "0" values where no precipitation was recorded. This would be particularly prevalent during the dry season in Namibia, when rainfall is rare. In addition to the Mann Kendall Test, a Theil-Sen estimator was also used to calculate the slope values for the non-parametric trends. While not all the months were expected to necessarily have data that are non-normal, it was important to analyze the data in a uniform manner so that a comparison between different months would be possible.

For the months of March through August, few if any significant trends are evident in TRMM. September shows a significant increase; however the trends show the annual changes are all less than 1 mm/year (Figure 4.15). In October, there are five data points that have a significant decreasing trend greater than 2 mm/year. Between November and February inclusive, February is the only month when there are numerous significant trends: TRMM shows an increasing trend in a northwest to southeast strip inland from the Namibian coastline. Because most months in the baseline dataset recorded either minor significant trends or no significant trends at all, February is the only month for which trend differences between the datasets are discussed.

There are no significant trends for the ERA dataset in the month of February (Figure 4.16). The CPC dataset has two small regions of significance along the

Figure 4.14. The 1998-2013 annual precipitation trends for TRMM (upper left), CRU (upper right), ERA (lower left), and CPC (lower right) given in mm/year.

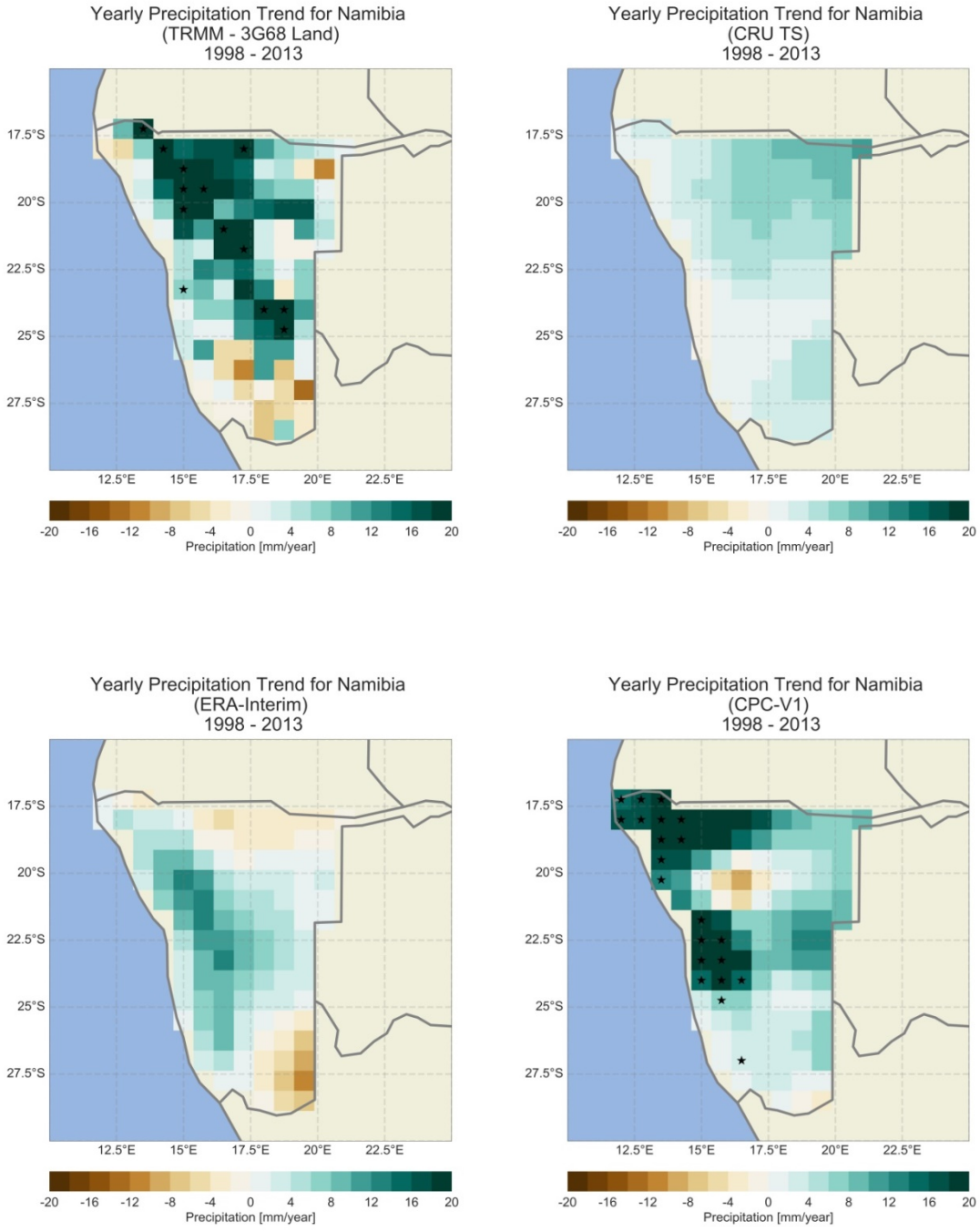

Figure 4.15. The monthly precipitation trend maps for February (left), September (center), and October (right) given in mm/year. February and September extend to 2014, October extends to 2013.

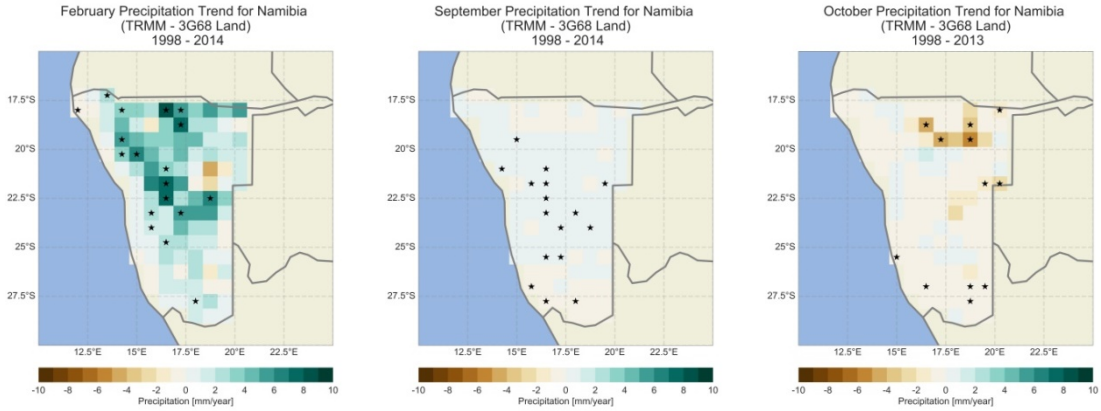

Namibian coastline. The northernmost region has a significant trend as high as 5 mm/year. The central region is smaller with a maximum trend of 3 mm/year. Between the two regions trends in only four data cells correspond to trends in TRMM.

The CRU dataset has a large region of significant positive precipitation trends in northwestern Namibia that extends from the northern Namibian coastline inland towards northern-central Namibia. The maximum trend evident over the region of significance is 7 mm/year. The significant trends evident in the CRU dataset align somewhat with the sporadic significant trends that are evident in TRMM. Six data cells between the two datasets have significant positive trends at the same location.

4.1.4. Conclusion

The results of the spatial and temporal analyses provide different perspectives of the overall precipitation comparison. The spatial analyses showed that CRU was the best

Figure 4.16. The February Precipitation Trend Maps from 1998-2014 for TRMM (upper left), CRU (upper right), ERA (lower left), and CPC (lower right) given in mm/year.

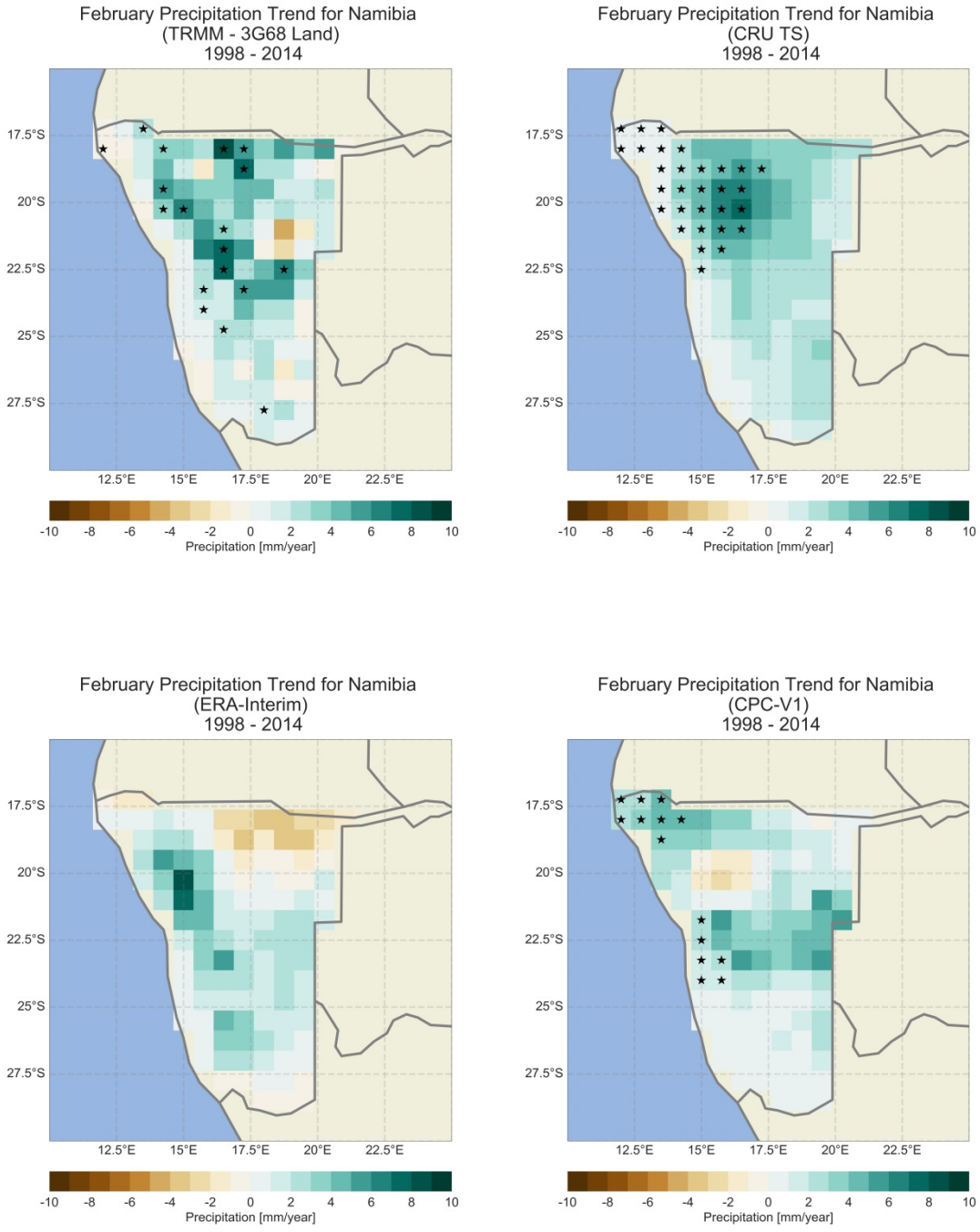

product when compared against the TRMM baseline. ERA came in a close second place for the spatial analyses. CPC was the worst of the three products in the spatial analyses. While the results of the spatial analyses have CRU as the best product, the results change when considering the temporal analyses. Analyzed over the entire country as well as numerous basins, the results suggest that CRU does not perform as well as ERA. In addition, the deciding factor proved to be the results of the Kunene Basin analysis. Artifacts in the CRU dataset that are likely due to the use of fill values for data-sparse areas proved that CRU would not be appropriate for further analyses that required a time series that did not use fill values. Because of this, ERA was chosen as the best product for creating a long-term climatology and trend analysis, as well as identifying global drivers of Namibian precipitation.

4.2. Namibia's Precipitation Climatologies and Trends

While the ERA-Interim dataset starts in January of 1979, the last year of the 1970s was eliminated from analysis, with all analysis starting in January of 1980. The analysis ends in December of 2016. With thirty-seven years of data, climatologies and trend analyses for different time periods were created. Annual, monthly, rainy season, and dry season periods were considered. The study period extends over thirty years, a timespan generally thought to be the minimum length of time for suitable climatologies.

To provide a basic snapshot of Namibia's precipitation, boxplots were created to show the annual and seasonal cycle averaged across all of Namibia. The plots provide a sense for how rainfall changes from one month to the next in an average year, while also showing the variations and extremes (Figure 4.17).

Figure 4.17. Annual, rainy season, and dry season variations (top), with the annual precipitation cycle (bottom) for 1980 to 2016 using the ERA dataset. The 1st and 3rd quartiles are shown by the edges of the boxes, the whiskers represent the minimum and maximum temperatures, and the medians are plotted as horizontal lines with the boxes. The means are represented by the dots.

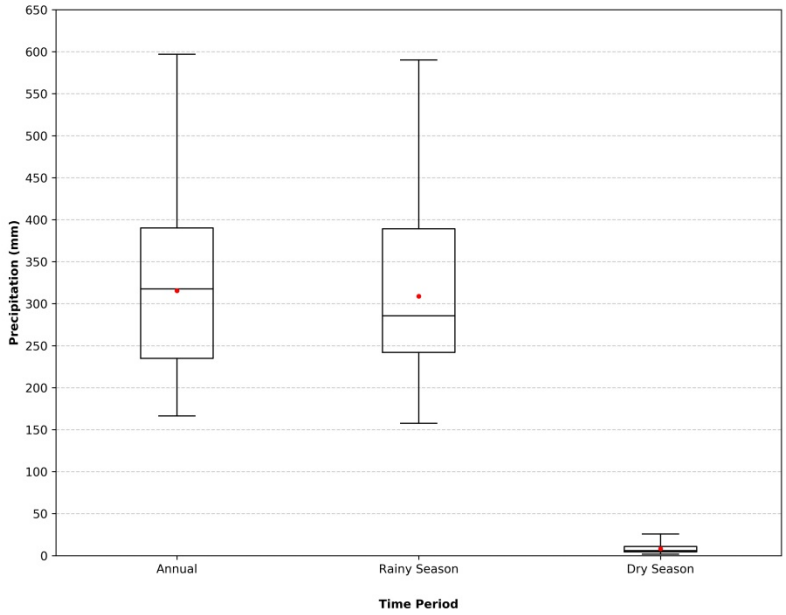

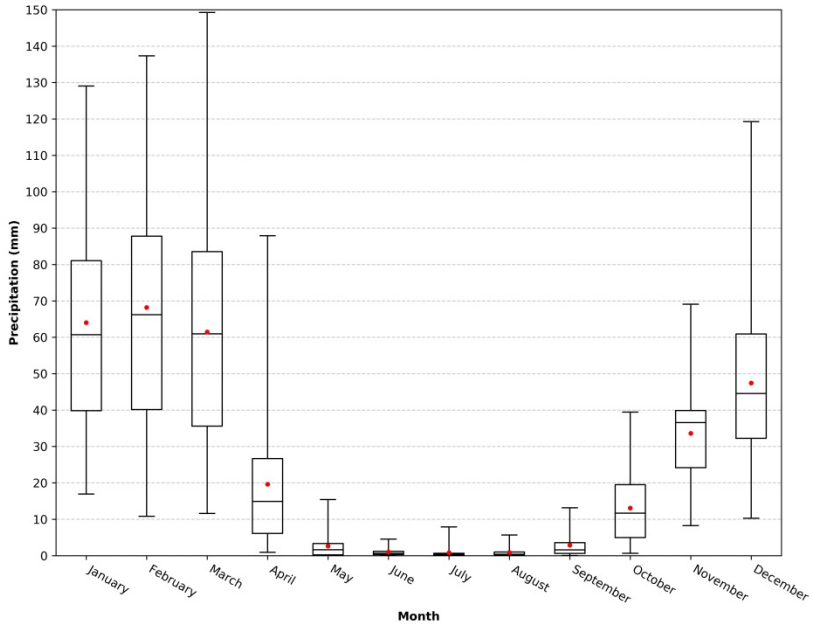

4.2.1. Climatologies

The annual climatology provides a clear depiction of the spatial precipitation pattern in Namibia during the period from 1980 to 2016 (Figure 4.18 – left). Annual precipitation averages above 600 mm stretch along the border with Angola in the eastern corner of the country. There is both a zonal and meridional decrease in precipitation extending out from the northeast corner of the country. The Namibian coastline is dry, with the Namib Desert evident along much of the coastline. The precipitation decreases that are evident inland follow a north-south pattern. Annual precipitation levels as low as 120–150 mm are evident in southern Namibia, along the border with South Africa.

The monthly climatologies for Namibia illustrate the different aspects of the Namibian rainy season followed by the long and quite uniform Namibian dry season. The Namibian rainy season starts in October, with virtually no precipitation evident along the coastline, and the highest precipitation levels evident in the northeastern corner of the country (Figure 4.18 – center). The positive, southwest to northeast precipitation gradient is prevalent in the October climatology. The Namibian coastline sees between 0 – 7.5 mm of rainfall in the month of October, while the northeastern corner of Namibia sees as much as 22.5 – 30 mm. The gradient in northern Namibia is stronger than the more gradual gradient in the south.

In November, the precipitation gradient becomes more extreme (Figure 4.18 – right). Little change in precipitation is evident in southern Namibia in October versus November, with only a marginal increase in the northwestern corner of Namibia. This is juxtaposed to the precipitation increases evident in northeastern Namibia. The

precipitation levels that totaled no more than 30 mm in the month of October, increase to as much as 82.5 mm in November. The precipitation increase in the entire northeastern quadrant of Namibia is sizable, with most of the area that previously only saw between 15 – 22.5 mm of rainfall in October now experiencing no less than 22.5 mm of precipitation.

Figure 4.18. Annual precipitation climatology (left) and precipitation climatology for October (center), and November (right) for 1980 to 2016.

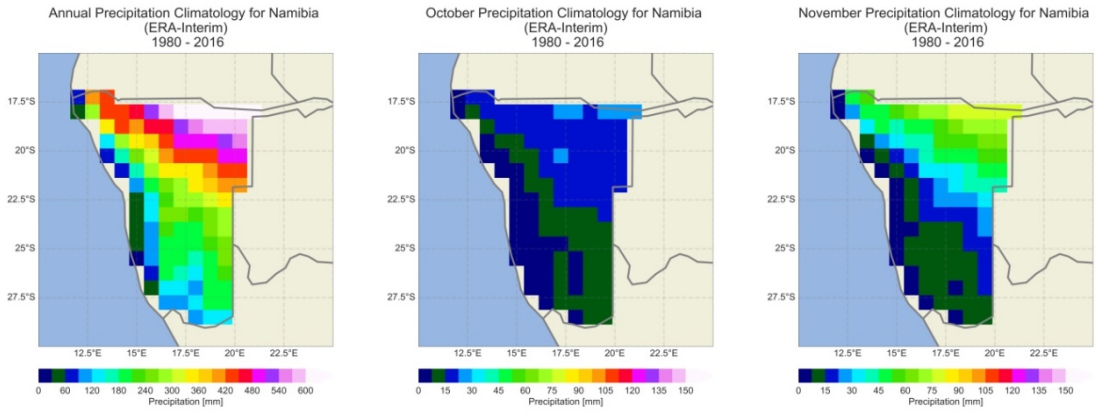

Continuing in to December, the October precipitation pattern continues (Figure 4.19 – left). A marginal increase in precipitation is evident in southern Namibia, with precipitation levels below 15 mm confined to the southernmost border of Namibia and the Namib Desert. However, the increases in precipitation in southern Namibia are still marginal relative to the increases seen in northern Namibia. The northeastern corner of Namibia that borders Angola and the Caprivi Strip have precipitation accumulations in December as high as 127.5 mm. Most of the northeastern quadrant of Namibia has precipitation levels above 45 mm, a substantial increase over November. Northwestern

Figure 4.19. Precipitation climatology for December (left), January (center), and February (right) for 1980 to 2016.

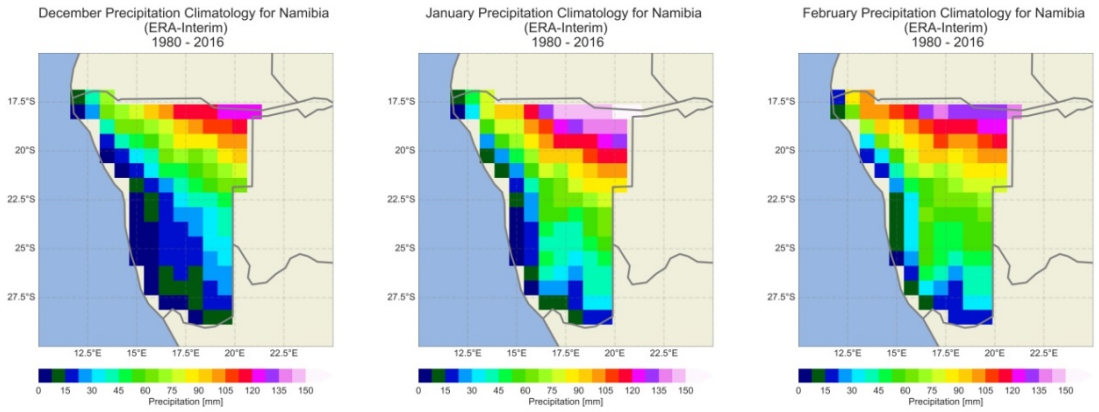

Figure 4.20. Precipitation climatology for March (left) and April (right) for 1980 to 2016.

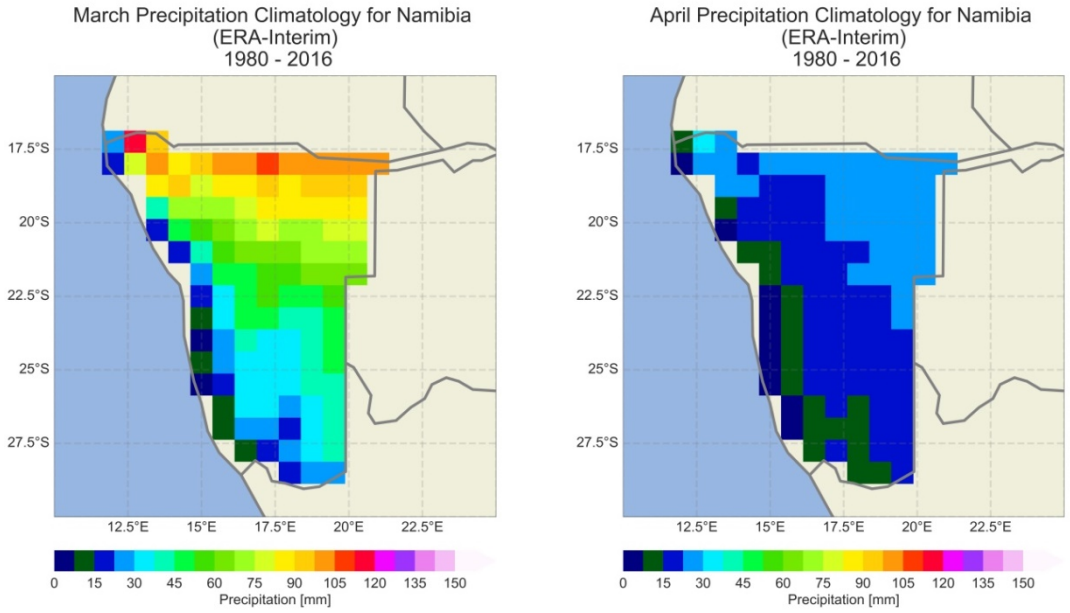

Namibia's precipitation gradient is extreme, with the coastline still seeing precipitation below 15 mm, but the land just inland experiencing precipitation as high as 45 mm. This demarcates the boundaries of the Namib Desert in northern Namibia.

January is the rainiest month in Namibia, with precipitation levels in the northeastern corner exceeding 150 mm (Figure 4.19 – center). The high levels of precipitation extend southwards, with parts of southeastern Namibia seeing rainfall as high as 45 mm. While the Namib remains quite dry, with almost the entire length of the coastline experiencing 22.5 mm of precipitation or less, the rest of Namibia experiences a noticeable increase in precipitation over the beginning of the rainy season in October.

Figure 4.21. Precipitation climatology for the dry (left) and rainy (right) seasons for 1980 to 2016. Note the different precipitation scale for the dry season.

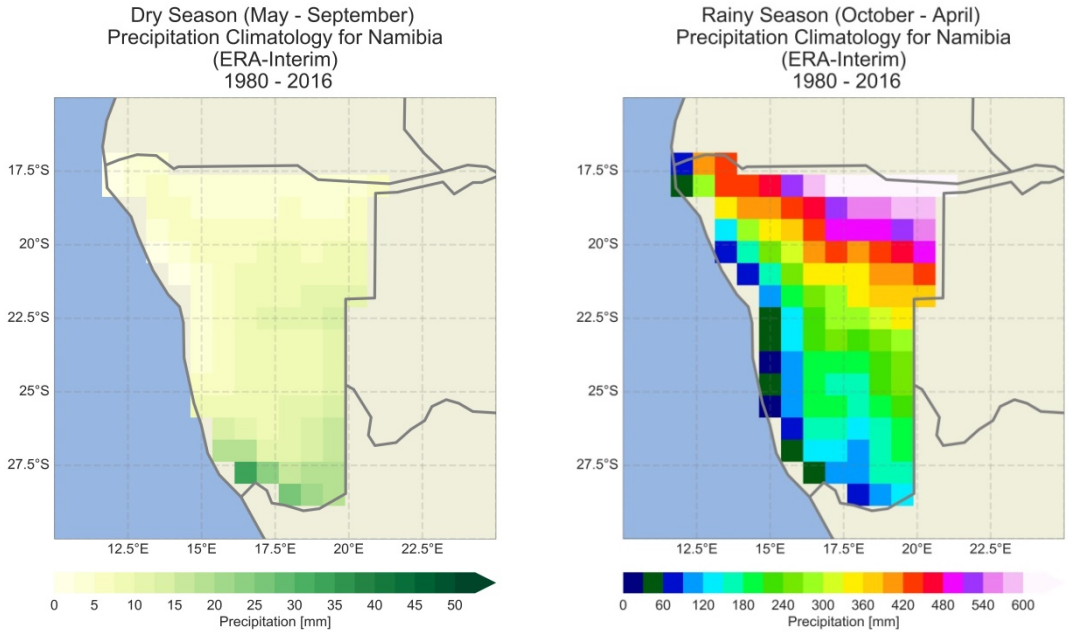

The northeastern quadrant of Namibia generally receives at least 75 mm of rainfall in the month of January, with much of the quadrant receiving over 100 mm of rainfall. January is the rainiest month in the rainy season and contributes much of precipitation that Namibia will see in a year.

By February, the highest monthly rainfall totals have decreased somewhat from January levels. Rainfall totals do not exceed 135 mm in any part of the country (Figure 4.19 – right). The gradient between precipitation in central and southern Namibia flattens out in February, with precipitation in central Namibia increasing and the precipitation in northeastern Namibia decreasing. Precipitation over the Namib Desert also sees an increase in rainfall compared to January, with almost the entire desert receiving at least 7.5 mm of rainfall. While precipitation in northeastern Namibia decreases in February, precipitation in northwestern Namibia increases. Areas that did not see precipitation exceed 82.5 mm in January experience precipitation accumulations as high as 105 mm in February. While there is still a decreasing northeast to southwest precipitation gradient, it is not nearly as strong as in January, and suggests a general shift towards a shrinking north to south precipitation gradient.

In March, the rainy season in Namibia starts to come to a close (Figure 4.20 – left). Compared to February, there is a decrease in precipitation across all of Namibia, with all but two data points recording less than 105 mm of precipitation in March. The diagonal precipitation gradient that was evident in the beginning of the rainy season has all but disappeared, with precipitation in the northeast of the country no longer higher than in the northwest. The dominant precipitation gradient transitions to a north/south

gradient, with the coastline still remaining arid. While precipitation levels decrease relative to February, the recorded amounts are still much higher than rainfall totals seen during the start of the rainy season, with some southern Namibian precipitation values as high as 45 mm.

April brings a significant drop in precipitation (Figure 4.20 – right). The last month of the rainy season, April has only one data point that exceeds 30 mm of precipitation. Similar to the northeastern quadrant of high precipitation that is evident at the beginning of the rainy season, higher precipitation is again evident in the northeastern quarter of Namibia. However, unlike at the onset of the rainy season, much of the country still sees between 15 and 30 mm of rainfall, with only the coastal areas and the southernmost portion of Namibia experiencing less than 15 mm of rainfall in April. With the end of April, the rainy season in Namibia comes to an abrupt close. Between the months of May and September, no portion of Namibia receives more than 7.5 mm of rainfall in any one month (not shown).

While the accumulated precipitation for the five month dry season is minimal, with only three grid cells receiving more than 25 mm of precipitation over the entire period, there is a different rainfall pattern evident in the dry season (Figure 4.21 – left). The highest precipitation occurs along the southern border with South Africa. There is an increasing precipitation gradient from north to south, with the lowest dry season values along the Angolan border and the Namibian coastline. The seven-month rainy season closely resembles the precipitation pattern seen in the annual precipitation

climatology (Figure 4.21 – right). This is expected because little precipitation occurs during the Namibian dry season.

4.2.2. Trends

An annual trend analysis was performed using a simple linear regression with the slope of the regressions providing the annual precipitation change (Figure 4.22 – left). There are significant precipitation increases across most of Namibia, with the exception of southern-most Namibia. The annual rate of change for precipitation in Namibia was as high as 8 mm/year over the thirty-seven year period, with the highest trends evident in northwestern Namibia. Trends as high 7 mm/year are widespread, with much of northern central Namibia seeing increases of between 6 to 7 mm/year. The rate of change generally decreases as latitude increases until there are almost no statistically significant cells.

Figure 4.22. Annual precipitation trend (left) and precipitation trends for November (center), and December (right) for 1980 to 2016.

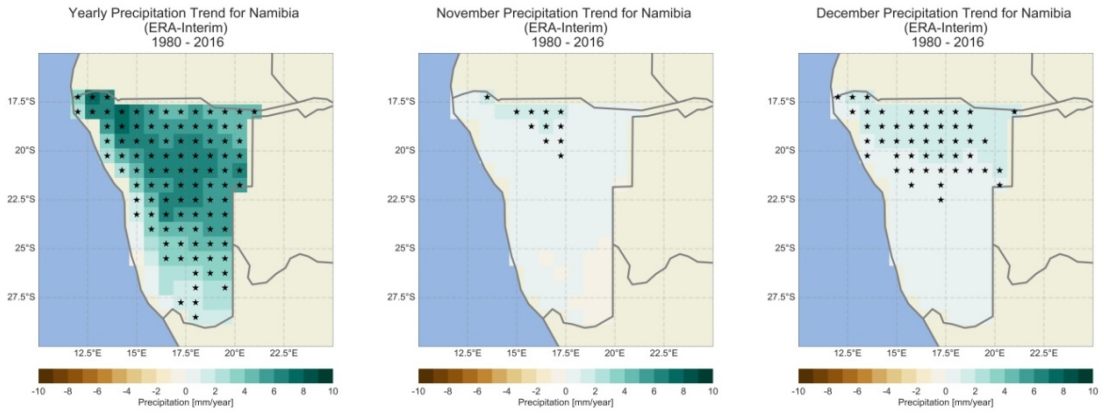

Based on the Mann-Kendall test, the first month of the rainy season to experience a significant trend is November (Figure 4.22 – center). While there are relatively few significant cells, they are all centrally located on the border with Angola. The Theil-Sen slopes indicate increases between 1-2 mm/year for that small region of northern Namibia.

By December, there is a sizable area with significant trends (Figure 4.22 – right). Much of the northern half of Namibia now has significant increases in precipitation that were not evident in November, including the entire region that had been significant in November. The increases in precipitation are modest, not exceeding 2 mm/year.

There is a considerable shift between the December and January trends (Figure 4.23 – left). Namibia's northern border and the coastal desert experience no significant changes in January, while the rest of Namibia sees increases between 1-3 mm/year. The highest precipitation increases are still evident in the northern half of Namibia.

While the seven-month rainy season continues until the end of April, the remaining rainy season trends only show significant precipitation increases in February and March, with no noticeable country-wide trends in April (Figure 4.23 – right; Figure 4.24 – left). The February trend analysis suggests that there is a significant increase in precipitation along the northern Namibian coastline. The precipitation increases along the coastline are between 1-2 mm/year, with only one data point recording a 3 mm/year rate. The March trend analysis is reminiscent of the January analysis, with much of the country seeing significant changes, instead of only a small region. Most of Namibia

north of 25°S experiences significant changes in precipitation, with trends between 1-3mm/year.

Figure 4.23. Precipitation trends for January (left) and February (right) for 1980 to 2016.

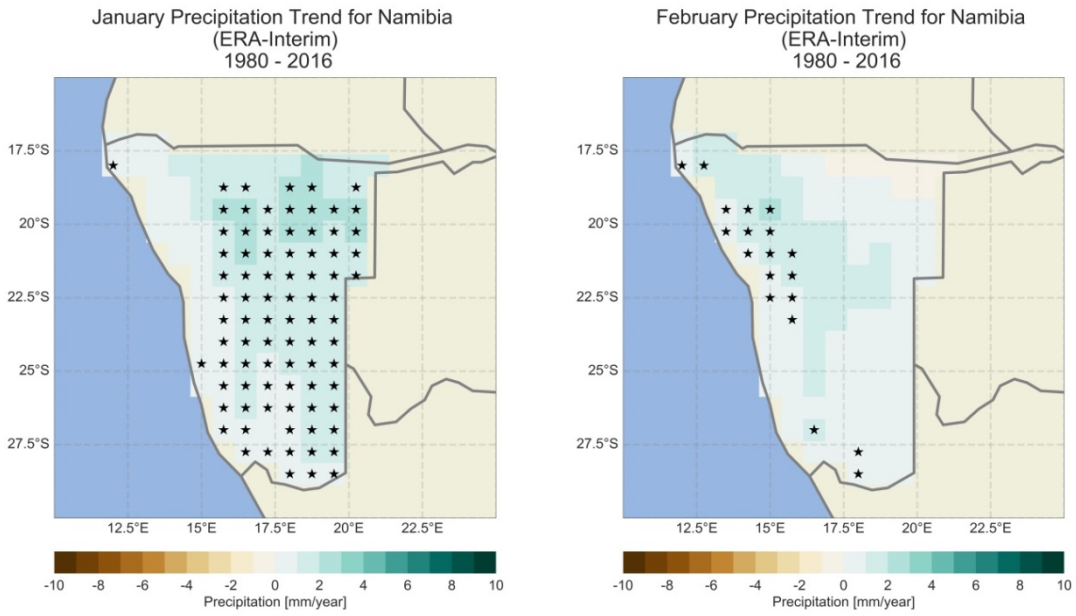

Starting in April, no significant precipitation trends are evident in Namibia until the start of the rainy season in October. While a couple significant grid cells are evident in the dry season, they are scattered across the country and suggest that Namibia has seen little monthly change in dry season precipitation over the last thirty-seven years (not shown).

Looking at the seven month rainy season that extends from October to April, the changes suggest that there was an annual increase in rainy season precipitation across

Namibia ranging between 1-7 mm/year (Figure 4.24 – right). No part of Namibia's southern border has experienced statistically significant precipitation changes over the thirty-seven year study period.

Figure 4.24. Precipitation trends for March (left) and the rainy season (right) for 1980 to 2016.

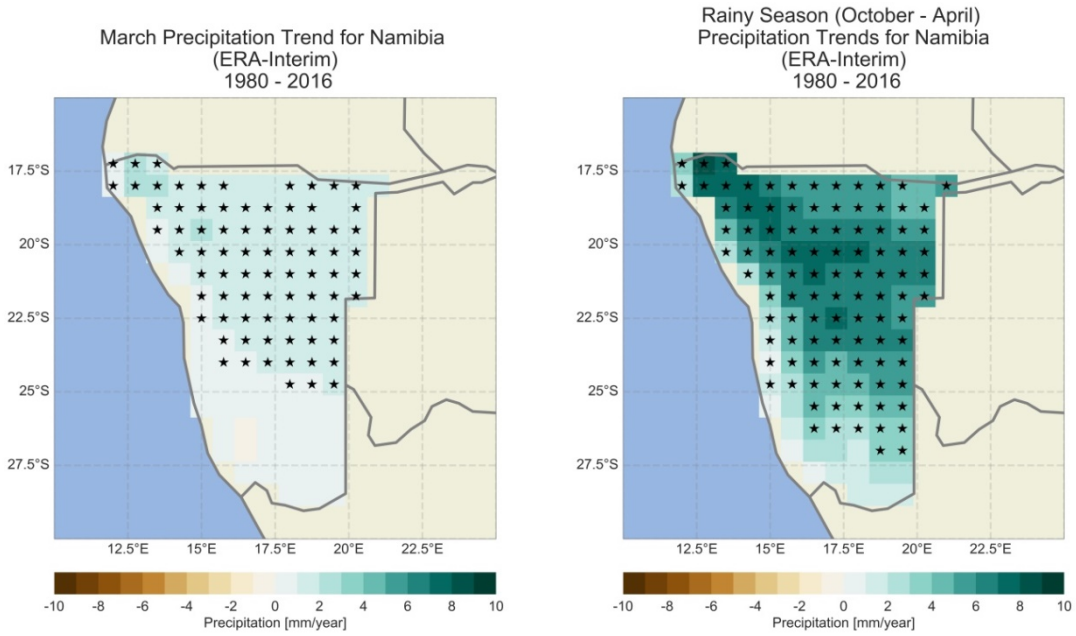

4.2.3. Conclusion

Precipitation climatologies for Namibia show the rainy season starting in October, with peak rainfall occurring in January. From January the precipitation decreases until the end of April, at which time the Namibian rainy season ends. The dry season begins in May and continues until September, with a negligible quantity of rainfall occurring during the dry season.

The annual trend analysis suggests that annual precipitation has increased in Namibia, especially in northern and central Namibia. Broken down in to monthly trend analyses, it seems that there have been significant monthly increases in precipitation over the thirty-seven year study period, with positive trends evident across much of Namibia during the months December, January, and March. Other than November and February, two months in which small portions of Namibia see positive precipitation trends, the remaining seven months of the year see virtually no change. The rainy season trend analysis suggests that the rainy season closely mimics the trends seen at the annual time scale.

4.3. Potential Drivers of Namibia's Precipitation

With an understanding of Namibia's temporal and spatial precipitation variability from 1980-2016, an important next step is to determine the potential causes of those patterns. This evaluation takes two forms. The first part considers the direct relationship between teleconnection indices and the gridded precipitation data. The second part of the evaluation utilizes a PCA to decrease the number of variables that need to be considered from 171 grid cells, to a small number of principal components. Only the first two principal components are considered, because the higher order principal components generally do not account for a significant percentage of the precipitation variance. Both methods are used to identify which teleconnections have the closest correlation to precipitation in Namibia, thereby providing support for what global climate patterns are potentially influencing precipitation over Namibia.

4.3.1. Teleconnection – Precipitation Correlations

Eleven teleconnections were evaluated at a monthly timescale (all twelve months individually), as well as over the full 444-month period. In addition to the different time periods, lag times from −6 months to +6 months inclusive were considered (for a total of 13 lag time periods). Spearman's Rank correlations were used to correlate precipitation values with the teleconnections. The monthly teleconnection – precipitation correlations found only three instances where more than ten grid cells were found with statistically significant Spearman correlations.

The first instance found a correlation between rainfall in October and NAO values four months later in February (Figure 4.25 – left). There is a four month lag time between when the precipitation occurred and when the NAO values were recorded (denoted as a -4 month lag time). There were 28 significant cells after a Bonferroni correction was applied to account for multiple comparison effects. The significant cells showed negative correlations between the NAO and rainfall in southern Namibia. This means that when there is decreased precipitation over Namibia in October, the NAO shifts to a positive phase by February of the next year. When there is increased precipitation over Namibia in October, the NAO shifts to a negative phase by February of the following year. Over fifteen of the 28 cells had negative correlations between -0.60 and -0.70.

Figure 4.25. Spearman correlation results for: October precipitation – February NAO [-4 lag] (left) March precipitation – November PDO [+4 lag] (center), and March precipitation – October PDO [+5 lag] (right) from 1980 to 2016.

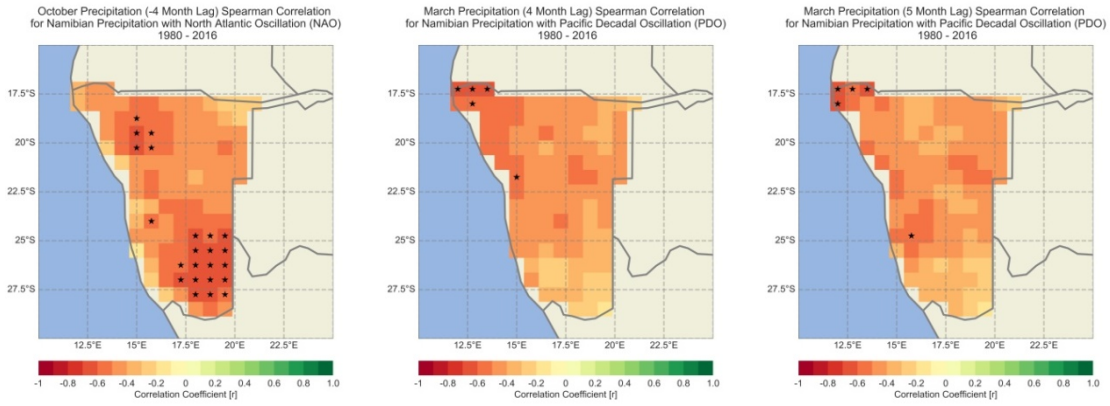

The second and third instances discovered correlations between rainfall in March and PDO values four and five months earlier in November and October (with 4 and 5 month lag times respectively) (Figure 4.25 – center; right). For the 4 month lag time, there were 11 cells that showed significant correlations to the PDO values. The negative correlations were in the northwestern corner of the country along, and extending over, the border with Angola. The negative correlation coefficients were generally between -0.60 and -0.70. With the 5 month lag time; there were 10 cells that showed significant correlation to the PDO. The location and strength of correlation for the significant cells was almost identical for both the 4 and 5 month lag times, with only slight differences.

In addition to the monthly correlations, a 444 month correlation was also considered. To remove the seasonality from the 444 month precipitation dataset, the values were standardized seasonally with respect to each month's mean and standard deviation (e.g., January months were standardized using only January values, etc.). The

444 month correlations were performed at the same lag times as the monthly data and for all eleven teleconnections. Nonetheless, none of the 444 month correlations saw 10 or more statistically significant cells.

4.3.2. Teleconnection – PCA Correlations

In the previous section, each grid cell was correlated with each teleconnection. In this section, the first two principal components of a PCA were correlated with each teleconnection. The use of principal components to discern which teleconnections drive precipitation over Namibia is effective, since it identifies the dominant modes of variability within a dataset by reducing the dimensions of the dataset.

Correlations are again performed with lag times from -6 months to +6 months. For example, if a PC from January is correlated with a (+6) teleconnection, that would mean that the PC is correlated with the teleconnection from the July six months prior. If a PC from January is correlated with a (-6) teleconnection, that would mean that the PC is correlated with the teleconnection the July six months later. This is done for all twelve months, the full 444 month period, and the seven month Namibian rainy season (October – April), for a total of 14 PCAs. The rainy season correlation was not calculated at multiple lag times with the teleconnections averaged over the rainy season period.

While over 300 different correlations were found to be significant, many had correlation values too low to be physically meaningful. To narrow the focus of the results, only correlations coefficients greater than 0.50 were evaluated further. PC correlations that were between 0.50 and 0.55 were also not evaluated, since second PC correlations already account for a smaller fraction of the variability. Additionally, two

significant first principal component correlations from September were not included because there was no noticeable change in precipitation between the positive mode and the negative mode of the PC.

Figure 4.26. Rainy season PC1 standardized loadings (left), with the composite positive (center) and negative (right) modes of precipitation from 1980 to 2016.

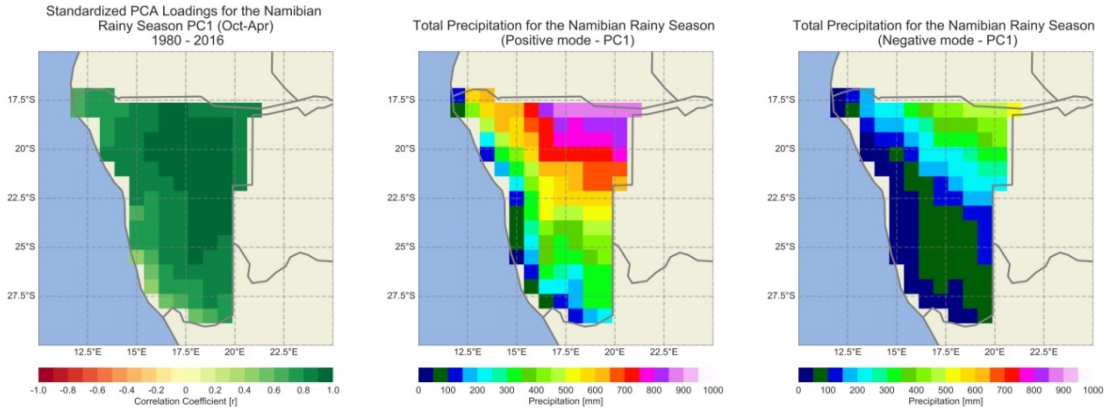

With a correlation coefficient of 0.57, the 1st principal component (PC) of the Namibian rainy season correlates significantly with the rainy season-averaged SOI. Loadings for eastern Namibia are predominantly above 0.90, while all but the coastal and southern-most regions of Namibia have loadings above 0.70 (Figure 4.26 – left). Further, by looking at averaged rainfall for years with the five highest and five lowest PC1 rainy season scores, the relationship between PC1 and rainfall is evident. In years when the PC scores were high, high rainfall occurs across Namibia (Figure 4.26 – center). While the coastal region remains relatively dry, inland Namibia sees precipitation levels above 300 mm, with northeastern Namibia experiencing precipitation totals reach as high as 900 mm. In years when the PC scores are low, low

precipitation is recorded across Namibia (Figure 4.26 – right). While precipitation remains low along the coastline as usual, inland precipitation decreases considerably, with almost half of Namibia seeing below 100 mm throughout the entire rainy season. Even in the wet, northeastern corner of Namibia, precipitation totals for the rainy season do not exceed 550 mm. This means that in years when SOI was in the positive mode, precipitation across Namibia would increase during the rainy season. In years when SOI was in the negative mode, precipitation in Namibia would decrease during the rainy season.

There is a significant correlation between PC1 precipitation in January and SOI values one month earlier in December (+1 lag), with a correlation of 0.52. The standardized loadings for January PC1 show high loading values in northern-central Namibia (>0.90), with all but the coastal regions characterized by loadings above 0.50 (Figure 4.27 – left). Rainfall averages from the years with the five highest and five lowest January PC1 scores are calculated. In years when the PC scores are high, high precipitation is evident over most of Namibia. Rainfall levels above 100 mm are evident across all but southern and coastal Namibia, with precipitation exceeding 200 mm evident in the northeastern quadrant of the country (Figure 4.27 – center). In years when the PC scores are low, low precipitation is found across the entirety of Namibia. Precipitation does not exceed 100 mm anywhere in Namibia, while most of the country sees below 20 mm of rainfall (Figure 4.27 – right). Thus when SOI was in the positive mode in December, precipitation across Namibia would see an increase one month later

in January. When SOI was in the negative mode in December, precipitation over Namibia would see a decrease one month later in January.

Figure 4.27. January PC1 standardized loadings (left), with the composite positive (center) and negative (right) modes of precipitation from 1980 to 2016.

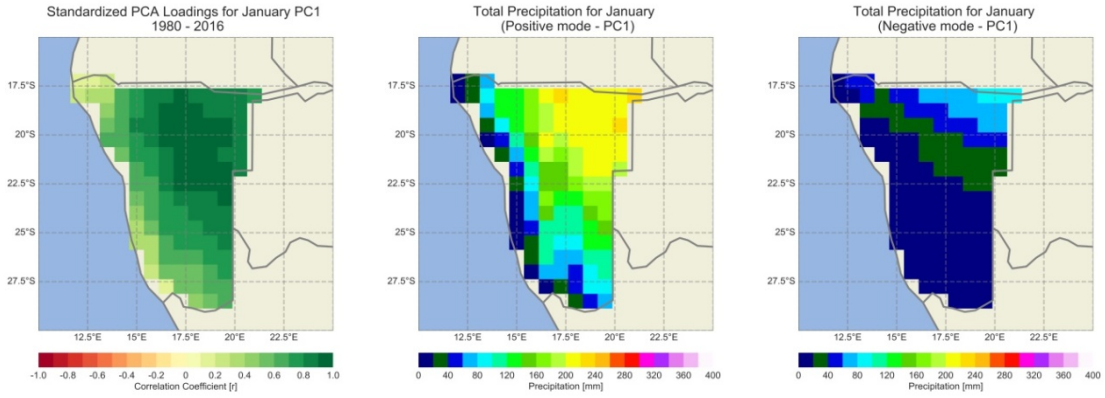

There are significant positive correlations between PC1 precipitation in February and SOI values in February (0 lag), January (+1 lag), December (+2 lag), November (+3 lag), and October (+4 lag), with correlation coefficients between 0.50 and 0.58. There is also a significant negative correlation between PC1 precipitation in February and PDO values four months earlier in October (+4 lag). Evaluating the spatial pattern for February PC1, there are high loadings across Namibia. The entire country has loadings above 0.50, with all but the Namibian coastline having loadings above 0.70 (Figure 4.28 – left). Rainfall averages from the years with the five highest PC scores indicate high precipitation throughout Namibia. Most of Namibia records precipitation between 100 and 200 mm, with the highest precipitation in northwestern Namibia, close to the Namibian coastline (Figure 4.28 – center). In years when the PC scores are low, low

precipitation is recorded. All but northern Namibia receives less than 20 mm of rainfall, with the highest accumulations in northeastern Namibia seeing no more than 60 mm (Figure 4.28 – right).

Figure 4.28. February PC1 standardized loadings (left), with the composite positive (center) and negative (right) modes of precipitation from 1980 to 2016.

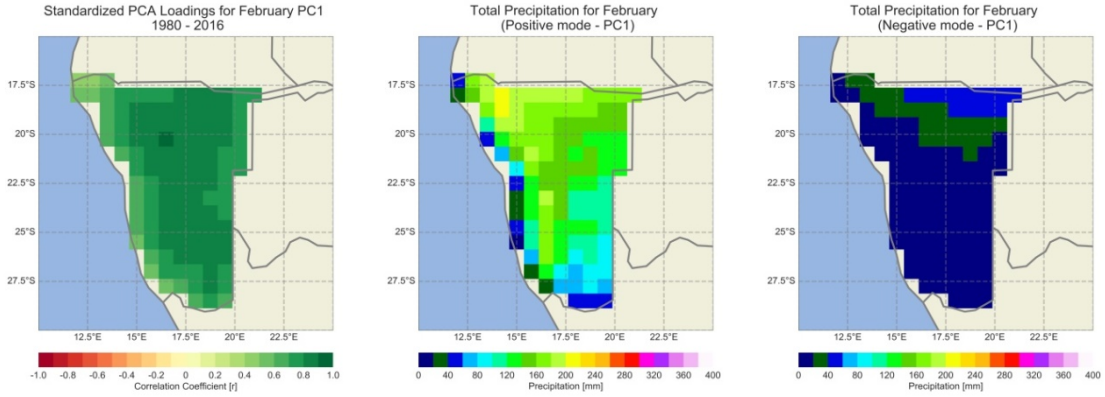

Therefore, in years when SOI was in the positive mode in October, November, December, January, and February, four to zero months later there is an increase in precipitation over Namibia. In years when SOI was in the negative mode in October, November, December, January, and February, four to zero months later, there would be a decrease in precipitation across Namibia. Additionally, in years when the PDO was in its positive phase in October, there was a decrease in precipitation four months later in February in Namibia. In years when the PDO was in its negative phase in October, there was an increase in precipitation four months later in February over Namibia.

4.3.3. Conclusion

The Spearman correlation between precipitation over Namibia and eleven teleconnections showed that there were only three instances where multiple grid cells had significant correlations with precipitation in Namibia. The instance with the most significant grid cells showed a negative relationship between October precipitation in southern Namibia and the NAO four months later in February. An increase in Namibian precipitation in October begets a negative NAO and vice versa. Because it is not expected that rainfall in Namibia is "forcing" the NAO, the results could either be spurious or suggest that something is forcing both precipitation in Namibia and the NAO. The remaining two instances showed negatives correlations between PDO values in November and December, and precipitation in Namibia four to five months later in March. The negative correlation means that the negative PDO phase correlates with increased precipitation, and vice versa.

The Pearson correlations between 1st and 2nd PCs of Namibian precipitation and eleven teleconnections, showed multiple instances of significant correlations, however only eight correlations had correlation coefficients and loadings that suggested they affect precipitation across all of Namibia. SOI was the best example of this with significant correlations above 0.50 evident at seven different time lags. Five of the seven periods showed a strong positive correlation between SOI values from October to February and rainfall in February, where a positive SOI mode from October to February leads to an increase in precipitation February and a negative SOI mode from October to February leads to a decrease in precipitation over Namibia in February. The sixth

instance showed a correlation between December SOI values and January precipitation where the positive mode of SOI in December leads to an increase in Namibian rainfall one month later in January. A negative mode of SOI in December conversely leads to a decrease in Namibian rainfall in January. The seventh showed a correlation between SOI values averaged over the rainy season and rainy season precipitation. The correlation shows that when the SOI is in a positive phase during the rainy season, from October to April, that there will be an increase in precipitation in Namibia over the same period. Conversely, when the SOI is in a negative phase during the rainy season, there will be a decrease in rainy season precipitation over Namibia. Last, PDO values in October were found to have a significant negative correlation to precipitation in February. Thus when the PDO is in a negative phase in October, there is an increase in precipitation over Namibia four months later in February. Likewise, when the PDO is in a positive phase in October, there is a decrease in precipitation over Namibia in the following February.

5. DISCUSSION

5.1. Precipitation Comparison

This study found ERA-Interim to best capture precipitation variability when compared against observations, as represented by TRMM. The spatial comparison results clearly showed that CPC performed poorly in representing precipitation over Namibia compared to the other two datasets. The trend analyses generally showed the same result, with ERA and CRU coming in almost tied and CPC lagging behind. The process of choosing between CRU and ERA was heavily dependent upon the sub-region (river basin) analyses. With the identification of irregularities in the Kunene river basin annual time series for CRU, and a general poor performance of the CRU dataset based on the RMSE, MAE, ME, and Spearman metrics, ERA emerged as the best data product to represent precipitation variability in this data-sparse, dry (arid and semi-arid) climate region.

The comparison of different precipitation products is common research topic, but nonetheless complicated in regions such as Namibia where there are little in situ data. For this reason, TRMM was chosen as the baseline dataset for this study. While South Africa still has an extensive gauge network, the Namibian gauge network is incredible limited and not usable as a baseline. While there are few studies that are directly comparable to this evaluation in Namibia, other studies have compared different precipitation products, including ERA-Interim, in other regions or at a different spatial scale. For example, the findings of Fu et al. (2016) showed that when precipitation from

the NCEP-National Center for Atmospheric Research reanalysis was compared to precipitation from the ERA-Interim reanalysis over Australia, against an observational baseline, ERA-Interim proved to be better at simulating rainfall. The semi-arid to arid climate that stretches across much of Australia is generally similar to the climate in Namibia, and this thesis thus validates the results of Fu et al. (2016).

The issues that were discovered in the CRU dataset over Namibia, where the long-term mean was apparently used for locations where there was no data, suggests that caution should be used when applying this dataset in Namibia, particularly for any study that is performing a trend analysis. For example, a study by Zhang et al. (2013) compared numerous reanalysis products over southern Africa, extending as far north as the equator, using CRU TS 3.1 as the baseline dataset. However, because the number of gauge stations in Namibia is severely limited, it is not advisable to use CRU TS 3.1 as a baseline. The study found that the NOAA-CIRES 20th Century Reanalysis V2 (20CRv2) performed better than ERA-Interim over southern Africa. However, the study did specify issues with ERA-Interim over the Democratic Republic of the Congo, a region of high precipitation, but not over Namibia. It is also important to note that the spatial resolution of 20CRv2 is 2.0° x 2.0°, which is considerably coarser than the 0.75° x 0.75° used by ERA-Interim. Lin et al. (2014) evaluated global monsoon precipitation for five different reanalysis datasets, one of which was ERA-Interim, against GPCP data. The evaluation found that the ERA-Interim precipitation climatology and interannual variability was the best of the five reanalysis datasets.

To conclude, a recent study by Sun et al. (2018) compared 30 global precipitation products. The study found that the Climate Forecast System Reanalysis best reproduced precipitation at a regional scale. However, it is noted that the precipitation is at a much finer scale than other datasets, with a resolution of 38 km. The result of the precipitation comparison in this thesis, with ERA identified as the best product over Namibia, seems in relative agreement with the few studies that have evaluated which datasets perform the best in representing precipitation in Africa or in semi-arid and arid climatic regions in general.

5.2. Precipitation Climatologies and Trends

This study found the rainy season in Namibia to start in October, with monthly precipitation levels up to 30 mm. The precipitation gradient that characterizes the first half of the Namibian rainy season also emerges in October, with the monthly precipitation totals decreasing from northeast to southwest. By November the precipitation gradient gets more extreme, with the northeastern totals doubling to over 75 mm of rain, with limited changes in the southwest. In December, the Namibian rainy season is in full force. Rainfall in the north exceeds 120 mm in some areas, and perhaps even more importantly, precipitation starts to increase in southwestern Namibia. While the rainfall quantities in southern Namibia are still small, around 15 mm, it still provides the southern half of the country with the first rainfall in eight months. The Namibian rainy season peaks in January. The rainfall quantities are as high as 150 mm bordering the Caprivi Strip, and all but the coastline seeing 15 mm or more of rainfall. By February the rainy season has begun to slow, with the highest precipitation evident across the

country decreasing to 135 mm. Consequently, the decreasing gradient shifts from northeast to southwest, and instead becomes a decreasing north-to-south gradient (with the coastline still remaining quite dry). However, rainfall totals in the southern half of Namibia still experience some increases in February. March heralds the beginning of the end, with only a narrow strip of precipitation above 100 mm. The decreasing north-to-south precipitation gradient still holds, though it is no longer as extreme as in February. Finally, the precipitation levels plunge in April. The dry season returns, and rainfall does not exceed 30 mm across the country. The core months of the Namibian rainy season thus are December, January, and February. While November and March act as bounds to the core of Namibia's rainy season, they are not very similar. March experiences greater quantities of precipitation and has a north-south gradient, while November does not receive nearly as much rain and has a northeast-southwest gradient. October and April are the true rainy season/dry season transitions. While the precipitation patterns are vaguely different, the precipitation quantities are relatively similar with April seeing slightly greater quantities of rainfall.

The dry season is extreme. Over a five month period, total precipitation does not exceed 30 mm. However, the spatial pattern of the small quantity of rain that does fall is unique. It reverses the rainy season pattern with a south to north decreasing precipitation gradient, with the highest precipitation quantities evident in the south. However, the precipitation amount is still incredibly small, with the totals seen over the entire five month dry season the same as October, the first month of the rainy season.

Other studies that have utilized and/or created precipitation climatologies over Namibia have found similar results (Foissner et al., 2002, Eckardt et al., 2013, Lu et al., 2016). However, it is important to reiterate that while other studies have found similar results, the scope of those studies was generally either localized to a small portion of Namibia, or regionalized to all of southern Africa. No other study previously explicitly focused on precipitation across all of Namibia.

The trend analyses in this study suggest that precipitation is increasing on an annual scale. Annual precipitation increases in Namibia extend from 1 to 10 mm/year. The highest increases are in northwestern and central Namibia, with relatively little change evident in southern Namibia. At the monthly scale, precipitation is increasing in certain rainy season months, but not for the rest of the year. Increases of 1-3 mm/year are evident in January and March. The increases in January are evident in almost all of the country except the northeast, while the increases evident in March are primarily evident in northern and central Namibia, instead of the south. December has increases of 1-2 mm/year in the northern half of Namibia. The rest of the months experience virtually no change in precipitation. The trends evident for the rainy season are almost identical to the annual trend, which is expected considering that the climatologies showed how the rainy season precipitation dominates Namibia's rainfall. Previous findings on precipitation trends across Namibia have varied. A study by Onyutha (2018) found that from 1961-1990, precipitation over northern Namibia was decreasing in the December/January/February months, but increased in the months of March/April/May during 1991-2015. While the differences in time period make a direct comparison

difficult, it should be noted that an increasing trend was found in this thesis (1980 to 2016) for the months of December, January, and March. Consequently, a study by Jury (2013) found there was an increasing trend (1979-2010) according to the ERA-Interim dataset. However, Jury (2013) also notes that the Institut Pierre Simon Laplace 20C dataset found there to be a decreasing trend over the same period that ERA-Interim found there to be an increasing trend. This does suggest some disagreement between datasets regarding the precipitation trends over southern Africa.

5.3. Potential Drivers of Namibia's Precipitation

To determine what influences the observed spatial and temporal patterns of precipitation variability in Namibia, two comparisons of eleven teleconnections to Namibian precipitation were performed. The first comparison was a direct correlation of the teleconnections to individual precipitation grid cells. This study found one case of significant correlations over a sizable region of Namibia, however the correlation suggested that October precipitation negatively correlates with NAO index values four months later in February. However, the timing of the rainfall and the NAO shows that the NAO is found respond to precipitation over Namibia. While interesting, this is not informative on what potentially drives precipitation variability in Namibia.

While the direct teleconnection – precipitation correlations did not find any significant relationships, the teleconnection – PCA correlations were much more insightful. The SOI was found to have a strong positive correlation to precipitation in the month of February. This relationship can be better understood with the framework of ENSO, where a positive SOI usually occurs in phase with La Niña and a negative SOI

usually occurs with El Niño. The correlation found in this study suggests that the occurrence of La Niña correlates with an increase in precipitation over Namibia, while El Niño correlates with a decrease in precipitation over Namibia. The literature appears to support these findings. Lindesay (1988), who looked at the relationship between the SOI and precipitation, found that in portions of South Africa during the austral summer rainy season, there was a positive correlation with the SOI. While this was over South Africa and not Namibia, the connection between summer rainy seasons (rather than winter rainy seasons) and the SOI high phase suggest that the relationship holds true over Namibia too. Mason and Jury (1997) suggest that in years with increased summer precipitation over southern Africa, there is a strong northeasterly inflow of moisture that provides the necessary ingredient for heavy summer rainfall. When there is a weak northeasterly inflow off the east coast of southern Africa, moisture from the Indian Ocean is not pushed across the continent. Dieppois et al. (2016) suggest that shifts in the Walker Circulation, forced by the La Niña phase of ENSO, move the SICZ over the African continent, where this source of moisture feeds the convection over Namibia during high SOI periods. The relationship between SOI and precipitation in southern Africa has been found to be strongest when both phases ENSO directly influence SST in the Atlantic and Indian Oceans (Nicholson, 2001). However, Nicholson (2001) did note that the relationship was more consistent during El Niño, with a decrease in precipitation over southern Africa, versus a less consistent relationship during La Niña, where precipitation over southern Africa did not always increase. Further understanding of how nearby SSTs in the southeastern Atlantic Ocean or southwestern Indian Ocean play a

role could be an avenue for future research. It is also interesting to note that while numerous El Niño teleconnections were correlated against precipitation in Namibia, none of them had correlation coefficients above 0.50. Only the Southern Oscillation component of ENSO was found to correlate strongly with Namibian precipitation. Additional research would be necessary to fully elucidate the relationship. Dieppois et al. (2016) found both phases of ENSO to interact with and potentially force the PDO. The negative correlation between the PDO and rainfall, where a positive PDO is associated with a decrease in precipitation over Namibia, while a negative PDO is associated with an increase in precipitation, was noted in this study.

6. CONCLUSION

In a region with high precipitation variability, a sparse population of people, and a large population of wildlife, it is important to know what the primary drivers of precipitation variability are (Turner et al., 2017). The unique nature of Namibia's climate also makes this study of particular importance. Positioned under the sinking air from the Hadley Cell and low SST from the Benguela current, Namibia holds a distinct place within the global climate system. And while numerous studies have looked at southern African precipitation as a whole, there is little information about precipitation over Namibia. The goal of this study was quantify Namibia's precipitation regime, with particular interest dedicated to better understanding what drives the precipitation in a region with such high variability.

The first objective of this thesis was to find the long-term dataset that best captures precipitation variability over Namibia. To do this, a shorter baseline dataset was used to identify the best long-term dataset. After utilizing multiple evaluation metrics, ERA-Interim was determined to be the precipitation dataset that best reproduces observed precipitation. The ERA product was then utilized for further analyses, from 1980 to 2016 at its original 0.75° x 0.75° spatial resolution and at a monthly, seasonal, and annual temporal resolution.

The second objective was to create precipitation climatologies and trend analyses at different timescales that show the spatial and temporal variability of precipitation in Namibia. The ERA-Interim climatologies showed a rainy season that normally starts in

October, peaks in January, and ends in April. The dry season extends from May until September. The trends showed that precipitation was increasing on an annual timescale by as much as 8 mm per year. The increases were also evident at a monthly timescale, with most of the increases evident in the middle to end of the rainy season.

The third objective was to utilize the ERA-Interim dataset and numerous major climate oscillations and global climatic patterns to identify what influences precipitation in Namibia. The final objective identified the SOI, and to some extent, the PDO, as affecting precipitation over Namibia. The effects of the SOI and PDO were most evident over Namibia in the months of February and January respectively. The correlation between the teleconnections and precipitation were strongest at the 4-month time lag, with teleconnection values from October correlating with precipitation in February.

The core months of the rainy season are December, January and February. Most of the rainfall that Namibia will experience in a year falls during that three month period. The spatial pattern of the rainy season shifts from a northeast to southwest decreasing precipitation gradient in the first half of the rainy season (October, November, December, and January), to a north to south decreasing precipitation gradient in the second half of the rainy season (February, March, and April). Precipitation increases over Namibia both at the annual time scale, and at a monthly time scale in the months of December, January, and March. The strongest drivers of Namibia's precipitation in this study are found to be the SOI and, to a lesser extent, PDO. There are still gaps in understanding how precipitation over Namibia occurs. While the trends calculated in this study show that precipitation is increasing in Namibia, it does not explain how that

precipitation is actually occurring. If the magnitude of precipitation has increased, but the actual number of precipitation events is decreasing, the effects of increased precipitation could be quite different from numerous, low magnitude precipitation events. Identifying the type and frequency of individual precipitation events is not possible without looking at precipitation data at a finer temporal resolution.

With ocean and atmospheric teleconnections playing a primary role in this thesis, it must be noted that conditions on the ground, such as vegetation and terrain, were not considered. Future research will potentially consider whether or not conditions on the ground play a significant role in precipitation variability, and if they do, how that relationship changes at different spatial and temporal scales. The importance of understanding precipitation over Namibia plays an important role in preserving and promoting wildlife in the region and drives me to continue my study of this arid region of southern Africa.

REFERENCES

AKINSANOLA, A. A., OGUNJOBI, K. O., AJAYI, V. O., ADEFISAN, E. A., OMOTOSHO, J. A. & SANOGO, S. 2017. Comparison of five gridded precipitation products at climatological scales over West Africa. *Meteorology and Atmospheric Physics,* 129**,** 669-689.

ASHOK, K., BEHERA, S. K., RAO, S. A., WENG, H. Y. & YAMAGATA, T. 2007. El Nino Modoki and its possible teleconnection. *Journal of Geophysical Research-Oceans,* 112**,** 27.

BELO-PEREIRA, M., DUTRA, E. & VITERBO, P. 2011. Evaluation of global precipitation data sets over the Iberian Peninsula. *Journal of Geophysical Research-Atmospheres,* 116**,** 16.

CHEN, M. & XIE, P. 2008. 3.3 Quality Control of Daily Precipitation Reports at NOAA/CPC.

CHEN, M. Y., SHI, W., XIE, P. P., SILVA, V. B. S., KOUSKY, V. E., HIGGINS, R. W. & JANOWIAK, J. E. 2008. Assessing objective techniques for gauge-based analyses of global daily precipitation. *Journal of Geophysical Research-Atmospheres,* 113**,** 13.

CONTRACTOR, S., ALEXANDER, L. V., DONAT, M. G. & HEROLD, N. 2015. How Well Do Gridded Datasets of Observed Daily Precipitation Compare over Australia? *Advances in Meteorology***,** 1-15.

COOK, K. H. 2000. The South Indian convergence zone and interannual rainfall variability over southern Africa. *Journal of Climate,* 13**,** 3789-3804.

COOK, K. H. 2001. A Southern Hemisphere wave response to ENSO with implications for southern Africa precipitation. *Journal of the Atmospheric Sciences,* 58**,** 2146-2162.

COSTA, M. H. & FOLEY, J. A. 1998. A comparison of precipitation datasets for the Amazon basin. *Geophysical Research Letters,* 25**,** 155-158.

CRETAT, J., POHL, B., RICHARD, Y. & DROBINSKI, P. 2012. Uncertainties in simulating regional climate of Southern Africa: sensitivity to physical parameterizations using WRF. *Climate Dynamics,* 38**,** 613-634.

DEE, D. P., UPPALA, S. M., SIMMONS, A. J., BERRISFORD, P., POLI, P., KOBAYASHI, S., ANDRAE, U., BALMASEDA, M. A., BALSAMO, G., BAUER, P., BECHTOLD, P., BELJAARS, A. C. M., VAN DE BERG, L., BIDLOT, J., BORMANN, N., DELSOL, C., DRAGANI, R., FUENTES, M., GEER, A. J., HAIMBERGER, L., HEALY, S. B., HERSBACH, H., HOLM, E. V., ISAKSEN, L., KALLBERG, P., KOHLER, M., MATRICARDI, M., MCNALLY, A. P., MONGE-SANZ, B. M., MORCRETTE, J. J., PARK, B. K., PEUBEY, C., DE ROSNAY, P., TAVOLATO, C., THEPAUT, J. N. & VITART, F. 2011. The ERA-Interim reanalysis: configuration and performance of the data assimilation system. *Quarterly Journal of the Royal Meteorological Society,* 137**,** 553-597.

DIEPPOIS, B., POHL, B., ROUAULT, M., NEW, M., LAWLER, D. & KEENLYSIDE, N. 2016. Interannual to interdecadal variability of winter and summer southern African rainfall, and their teleconnections. *Journal of Geophysical Research-Atmospheres,* 121**,** 6215-6239.

DYER, T. G. J. 1979. RAINFALL ALONG THE EAST COAST OF SOUTHERN-AFRICA, THE SOUTHERN OSCILLATION, AND THE LATITUDE OF THE SUB-TROPICAL HIGH-PRESSURE BELT. *Quarterly Journal of the Royal Meteorological Society,* 105**,** 445-451.

EBERT, E. E., JANOWIAK, J. E. & KIDD, C. 2007. Comparison of near-real-time precipitation estimates from satellite observations and numerical models. *Bulletin of the American Meteorological Society,* 88**,** 47-+.

ECKARDT, F. D., SODERBERG, K., COOP, L. J., MULLER, A. A., VICKERY, K. J., GRANDIN, R. D., JACK, C., KAPALANGA, T. S. & HENSCHEL, J. 2013. The nature of moisture at Gobabeb, in the central Namib Desert. *Journal of Arid Environments,* 93**,** 7-19.

ENFIELD, D. B., MESTAS-NUNEZ, A. M., MAYER, D. A. & CID-SERRANO, L. 1999. How ubiquitous is the dipole relationship in tropical Atlantic sea surface temperatures? *Journal of Geophysical Research-Oceans,* 104**,** 7841-7848.

FOISSNER, W., AGATHA, S. & BERGER, H. 2002. *Soil ciliates (Protozoa, Ciliophora) from Namibia (Southwest Africa), with emphasis on two contrasting environments, the Etosha region and the Namib Desert*, Biologiezentrum der Oberösterreichischen Landesmuseums.

FU, G. B., CHARLES, S. P., TIMBAL, B., JOVANOVIC, B. & OUYANG, F. 2016. Comparison of NCEP-NCAR and ERA-Interim over Australia. *International Journal of Climatology,* 36**,** 2345-2367.

GARSTANG, M., DAVIS, R. E., LEGGETT, K., FRAUENFELD, O. W., GRECO, S., ZIPSER, E. & PETERSON, M. 2014. Response of African Elephants (Loxodonta africana) to Seasonal Changes in Rainfall. *Plos One,* 9**,** 13.

HOELL, A. & CHENG, L. Y. 2018. Austral summer Southern Africa precipitation extremes forced by the El Nino-Southern oscillation and the subtropical Indian Ocean dipole. *Climate Dynamics,* 50**,** 3219-3236.

HOELL, A., FUNK, C., ZINKE, J. & HARRISON, L. 2017. Modulation of the Southern Africa precipitation response to the El Nio Southern Oscillation by the subtropical Indian Ocean Dipole. *Climate Dynamics,* 48**,** 2529-2540.

HURRELL, J. W. 1995. DECADAL TRENDS IN THE NORTH-ATLANTIC OSCILLATION - REGIONAL TEMPERATURES AND PRECIPITATION. *Science,* 269**,** 676-679.

JANOWIAK, J. E., GRUBER, A., KONDRAGUNTA, C. R., LIVEZEY, R. E. & HUFFMAN, G. J. 1998. A comparison of the NCEP-NCAR reanalysis precipitation and the GPCP rain gauge-satellite combined dataset with observational error considerations. *Journal of Climate,* 11**,** 2960-2979.

JONES, P. D., JONSSON, T. & WHEELER, D. 1997. Extension to the North Atlantic Oscillation using early instrumental pressure observations from Gibraltar and south-west Iceland. *International Journal of Climatology,* 17**,** 1433-1450.

JONES, P. W. 1999. First- and second-order conservative remapping schemes for grids in spherical coordinates. *Monthly Weather Review,* 127**,** 2204-2210.

JOYCE, R. J., JANOWIAK, J. E., ARKIN, P. A. & XIE, P. P. 2004. CMORPH: A method that produces global precipitation estimates from passive microwave and infrared data at high spatial and temporal resolution. *Journal of Hydrometeorology,* 5**,** 487-503.

JUAREZ, R. I. N., LI, W. H., FU, R., FERNANDES, K. & CARDOSO, A. D. 2009. Comparison of Precipitation Datasets over the Tropical South American and African Continents. *Journal of Hydrometeorology,* 10**,** 289-299.

JURY, M. R. 2013. Climate trends in southern Africa. *South African Journal of Science,* 109**,** 53-63.

KOKOT, D. F. 1948. *investigation into the evidence bearing on recent climactic changes over southern Africa,* Pretoria, Government Printer.

KUMMEROW, C., BARNES, W., KOZU, T., SHIUE, J. & SIMPSON, J. 1998. The Tropical Rainfall Measuring Mission (TRMM) sensor package. *Journal of Atmospheric and Oceanic Technology,* 15**,** 809-817.

LAMPTEY, B. L. 2008. Comparison of gridded multisatellite rainfall estimates with gridded gauge rainfall over west Africa. *Journal of Applied Meteorology and Climatology,* 47**,** 185-205.

LANDMAN, W. A., KGATUKE, M. J., MBEDZI, M., BERAKI, A., BARTMAN, A. & DU PIESANIE, A. 2009. Performance comparison of some dynamical and empirical downscaling methods for South Africa from a seasonal climate modelling perspective. *International Journal of Climatology,* 29**,** 1535-1549.

LEGGETT, K. E. A. 2006. Home range and seasonal movement of elephants in the Kunene Region, northwestern Namibia. *African Zoology,* 41**,** 17-36.

LIN, R. P., ZHOU, T. J. & QIAN, Y. 2014. Evaluation of Global Monsoon Precipitation Changes based on Five Reanalysis Datasets. *Journal of Climate,* 27**,** 1271-1289.

LINDESAY, J. A. 1988. SOUTH-AFRICAN RAINFALL, THE SOUTHERN OSCILLATION AND A SOUTHERN-HEMISPHERE SEMI-ANNUAL CYCLE. *Journal of Climatology,* 8**,** 17-30.

LINDESAY, J. A., HARRISON, M. S. J. & HAFFNER, M. P. 1986. THE SOUTHERN OSCILLATION AND SOUTH-AFRICAN RAINFALL. *South African Journal of Science,* 82**,** 196-197.

LINDESAY, J. A. & VOGEL, C. H. 1990. HISTORICAL EVIDENCE FOR SOUTHERN OSCILLATION SOUTHERN AFRICAN RAINFALL RELATIONSHIPS. *International Journal of Climatology,* 10**,** 679-689.

LU, X. F., WANG, L. X., PAN, M., KASEKE, K. F. & LI, B. N. 2016. A multi-scale analysis of Namibian rainfall over the recent decade - comparing TMPA satellite estimates and ground observations. *Journal of Hydrology-Regional Studies,* 8**,** 59-68.

MA, L. J., ZHANG, T., FRAUENFELD, O. W., YE, B. S., YANG, D. Q. & QIN, D. H. 2009. Evaluation of precipitation from the ERA-40, NCEP-1, and NCEP-2 Reanalyses and CMAP-1, CMAP-2, and GPCP-2 with ground-based measurements in China. *Journal of Geophysical Research-Atmospheres,* 114**,** 20.

MAIDMENT, R. I., GRIMES, D. I. F., ALLAN, R. P., GREATREX, H., ROJAS, O. & LEO, O. 2013. Evaluation of satellite-based and model re-analysis rainfall estimates for Uganda. *Meteorological Applications,* 20**,** 308-317.

MANTUA, N. J., HARE, S. R., ZHANG, Y., WALLACE, J. M. & FRANCIS, R. C. 1997. A Pacific interdecadal climate oscillation with impacts on salmon production. *Bulletin of the American Meteorological Society,* 78**,** 1069-1079.

MARCHANT, R., MUMBI, C., BEHERA, S. & YAMAGATA, T. 2007. The Indian Ocean dipole - the unsung driver of climatic variability in East Africa. *African Journal of Ecology,* 45**,** 4-16.

MASON, S. J. & JURY, M. R. 1997. Climatic variability and change over southern Africa: A reflection on underlying processes. *Progress in Physical Geography,* 21**,** 23-50.

MCCOLLUM, J. R. & FERRARO, R. R. 2003. Next generation of NOAA/NESDIS TMI, SSM/I, and AMSR-E microwave land rainfall algorithms. *Journal of Geophysical Research-Atmospheres,* 108**,** 23.

MCCOLLUM, J. R., KRAJEWSKI, W. F., FERRARO, R. R. & BA, M. B. 2002. Evaluation of biases of satellite rainfall estimation algorithms over the continental United States. *Journal of Applied Meteorology,* 41**,** 1065-1080.

MULLER, A., REASON, C. J. C. & FAUCHEREAU, N. 2008. Extreme rainfall in the Namib Desert during late summer 2006 and influences of regional ocean variability. *International Journal of Climatology,* 28**,** 1061-1070.

NICHOLSON, S. E. 2000. The nature of rainfall variability over Africa on time scales of decades to millenia. *Global and Planetary Change,* 26**,** 137-158.

NICHOLSON, S. E. 2001. Climatic and environmental change in Africa during the last two centuries. *Climate Research,* 17**,** 123-144.

NICHOLSON, S. E. & ENTEKHABI, D. 1986. THE QUASI-PERIODIC BEHAVIOR OF RAINFALL VARIABILITY IN AFRICA AND ITS RELATIONSHIP TO THE SOUTHERN OSCILLATION. *Archives for Meteorology Geophysics and Bioclimatology Series a-Meteorology and Atmospheric Physics,* 34**,** 311-348.

NICHOLSON, S. E. & ENTEKHABI, D. 1987. RAINFALL VARIABILITY IN EQUATORIAL AND SOUTHERN-AFRICA - RELATIONSHIPS WITH SEA-SURFACE TEMPERATURES ALONG THE SOUTHWESTERN COAST OF AFRICA. *Journal of Climate and Applied Meteorology,* 26**,** 561-578.

NICHOLSON, S. E. & KIM, E. 1997. The relationship of the El Nino Southern oscillation to African rainfall. *International Journal of Climatology,* 17**,** 117-135.

NICHOLSON, S. E. & SELATO, J. C. 2000. The influence of La Nina on African rainfall. *International Journal of Climatology,* 20**,** 1761-1776.

NIKULIN, G., JONES, C., GIORGI, F., ASRAR, G., BUCHNER, M., CEREZO-MOTA, R., CHRISTENSEN, O. B., DEQUE, M., FERNANDEZ, J., HANSLER, A., VAN MEIJGAARD, E., SAMUELSSON, P., SYLLA, M. B. & SUSHAMA, L. 2012. Precipitation Climatology in an Ensemble of CORDEX-Africa Regional Climate Simulations. *Journal of Climate,* 25**,** 6057-6078.

ONYUTHA, C. 2018. Trends and variability in African long-term precipitation. *Stochastic Environmental Research and Risk Assessment,* 32**,** 2721-2739.

RATNAM, J. V., BEHERA, S. K., MASUMOTO, Y. & YAMAGATA, T. 2014. Remote Effects of El Nino and Modoki Events on the Austral Summer Precipitation of Southern Africa. *Journal of Climate,* 27**,** 3802-3815.

REASON, C. J. C. 2001. Subtropical Indian Ocean SST dipole events and southern African rainfall. *Geophysical Research Letters,* 28**,** 2225-2227.

REASON, C. J. C. 2002. Sensitivity of the southern African circulation to dipole sea-surface temperature patterns in the south Indian Ocean. *International Journal of Climatology,* 22**,** 377-393.

REASON, C. J. C. & MULENGA, H. 1999. Relationships between South African rainfall and SST anomalies in the Southwest Indian Ocean. *International Journal of Climatology,* 19**,** 1651-1673.

ROUAULT, M., FLORENCHIE, P., FAUCHEREAU, N. & REASON, C. J. C. 2003. South East tropical Atlantic warm events and southern African rainfall. *Geophysical Research Letters,* 30**,** 1-4.

SAJI, N. H., GOSWAMI, B. N., VINAYACHANDRAN, P. N. & YAMAGATA, T. 1999. A dipole mode in the tropical Indian Ocean. *Nature,* 401**,** 360-363.

SAJI, N. H. & YAMAGATA, T. 2003. Possible impacts of Indian Ocean Dipole mode events on global climate. *Climate Research,* 25**,** 151-169.

SHANNON, L. V., BOYD, A. J., BRUNDRIT, G. B. & TAUNTONCLARK, J. 1986. ON THE EXISTENCE OF AN EL-NINO-TYPE PHENOMENON IN THE BENGUELA SYSTEM. *Journal of Marine Research,* 44**,** 495-520.

STANLEY, W. R. 2002. Namibia's unstable northern frontier. *Tijdschrift Voor Economische En Sociale Geografie,* 93**,** 369-382.

STROHBACH, B. J. 2008. Mapping the major catchments of Namibia.

SUN, Q. H., MIAO, C. Y., DUAN, Q. Y., ASHOURI, H., SOROOSHIAN, S. & HSU, K. L. 2018. A Review of Global Precipitation Data Sets: Data Sources, Estimation, and Intercomparisons. *Reviews of Geophysics,* 56**,** 79-107.

TESFAYE, T. W., DHANYA, C. T. & GOSAIN, A. K. 2017. Evaluation of ERA-Interim, MERRA, NCEP-DOE R2 and CFSR Reanalysis precipitation Data using Gauge Observation over Ethiopia for a period of 33 years. *Aims Environmental Science,* 4**,** 596-620.

THIEMIG, V., ROJAS, R., ZAMBRANO-BIGIARINI, M. & DE ROO, A. 2013. Hydrological evaluation of satellite-based rainfall estimates over the Volta and Baro-Akobo Basin. *Journal of Hydrology,* 499**,** 324-338.

THORNE, V., COAKELEY, P., GRIMES, D. & DUGDALE, G. 2001. Comparison of TAMSAT and CPC rainfall estimates with raingauges, for southern Africa. *International Journal of Remote Sensing,* 22**,** 1951-1974.

TRENBERTH, K. 2016. The climate data guide: Nino SST indices (Nino 1+ 2, 3, 3.4, 4; ONI and TNI). *Online, February*.

TRENBERTH, K. E. 1997. The definition of El Nino. *Bulletin of the American Meteorological Society,* 78**,** 2771-2777.

TRENBERTH, K. E. & STEPANIAK, D. P. 2001. Indices of El Nino evolution. *Journal of Climate,* 14**,** 1697-1701.

TRIPP, W. B. 1888. Rainfall of South Africa, 1842–1886. *Quarterly Journal of the Royal Meteorological Society,* 14**,** 108-123.

TURNER, W. C., KUSTERS, M., VERSFELD, W. & HORAK, I. G. 2017. Ixodid tick diversity on wild mammals, birds and reptiles in and around Etosha National Park, Namibia. *African Journal of Ecology,* 55**,** 714-721.

TYSON, P. D. & DYER, T. G. J. 1978. PREDICTED ABOVE-NORMAL RAINFALL OF SEVENTIES AND LIKELIHOOD OF DROUGHTS IN EIGHTIES IN SOUTH-AFRICA. *South African Journal of Science,* 74**,** 372-377.

TYSON, P. D., DYER, T. G. J. & MAMETSE, M. N. 1975. SECULAR CHANGES IN SOUTH-AFRICAN RAINFALL - 1880 TO 1972. *Quarterly Journal of the Royal Meteorological Society,* 101**,** 817-833.

VANHEERDEN, J., TERBLANCHE, D. E. & SCHULZE, G. C. 1988. THE SOUTHERN OSCILLATION AND SOUTH-AFRICAN SUMMER RAINFALL. *Journal of Climatology,* 8**,** 577-597.

WALKER, N. D. 1990. LINKS BETWEEN SOUTH-AFRICAN SUMMER RAINFALL AND TEMPERATURE VARIABILITY OF THE AGULHAS AND BENGUELA CURRENT SYSTEMS. *Journal of Geophysical Research-Oceans,* 95**,** 3297-3319.

WENG, H. Y., ASHOK, K., BEHERA, S. K., RAO, S. A. & YAMAGATA, T. 2007. Impacts of recent El Nino Modoki on dry/wet conditions in the Pacific rim during boreal summer. *Climate Dynamics,* 29**,** 113-129.

XIE, P. P., YATAGAI, A., CHEN, M. Y., HAYASAKA, T., FUKUSHIMA, Y., LIU, C. M. & YANG, S. 2007. A Gauge-based analysis of daily precipitation over East Asia. *Journal of Hydrometeorology,* 8**,** 607-626.

ZHANG, Q., KORNICH, H. & HOLMGREN, K. 2013. How well do reanalyses represent the southern African precipitation? *Climate Dynamics,* 40**,** 951-962.

ZHANG, Y., WALLACE, J. M. & BATTISTI, D. S. 1997. ENSO-like interdecadal variability: 1900-93. *Journal of Climate,* 10**,** 1004-1020.

ZHAO, T. B. & FU, C. B. 2006. Comparison of products from ERA-40, NCEP-2, and CRU with station data for summer precipitation over China. *Advances in Atmospheric Sciences,* 23**,** 593-604.